Development of the Gas Diffusion Layers to Improve the Lower and Higher Relative Humidity Performance of the Proton Exchange Membrane Fuel Cells

by

Nitin Chauhan

A Thesis Presented in Partial Fulfillment
of the Requirements for the Degree
Master of Science

Approved April 2021 by the
Graduate Supervisory Committee:

A M Kannan, Chair
Patrick Phelan
Qiong Nian

ARIZONA STATE UNIVERSITY

May 2021

ABSTRACT

Gas Diffusion Layers (GDL) based on PUREBLACK® carbon and VULCAN® (XC72R) carbon along with catalyst coated membranes were used to fabricate the membrane electrode assemblies for use in proton exchange membrane fuel cells (PEMFCs). Polyethylene glycol was used as the pore-forming agent on the microporous layer to improve the lower and higher relative humidity performance of the fuel cells. Accelerated stress tests based on the dissolution effect of GDLs were conducted and the long-term performance of the GDLs was evaluated. A single-cell fuel cell was used to evaluate the effect of porosity of the micro-porous layer and the effect of different types of carbon powder on the performance of the fuel cell at different operating relative humidity conditions and compared with commercial GDLs.

Both PUREBLACK® and VULCAN® (XC72R) based GDLs show crack-free surface morphology in the Scanning electron microscopy and hydrophobic characteristics in the contact angle measurements. The fuel cell performance is evaluated under relative humidity conditions of 60 and 100 % using H_2/O_2 and H_2/Air at 70 ℃ and the durability is also evaluated for the sample with and without 30% PEG for both carbons. The pristine PUREBLACK® based GDL sample with 30% pore-forming agent (total pore volume of 1.72 $cc.g^{-1}$) demonstrated the highest performance (peak power densities of 432 and 444 mW.cm-2 at 100 and 60 % RH respectively, using H_2/Air). There was a significant increase in the macropores when GDLs are aged in H_2O_2 and the contact angle dropped to about 14 and 95° for PUREBLACK® and VULCAN® carbon, respectively. Overall PUREBLACK® based GDLs performed the best after ageing both in H_2O_2 and H_2O (average performance degradation of 8% in H_2O_2 and 8.25% in H_2O).

ACKNOWLEDGMENTS

I would like to thank Dr. A. M. Kannan for his continuous guidance throughout the project. I appreciate the motivation and support he provided throughout the research. I would also like to thank Grigoria A. (PhD. candidate) for her valuable knowledge and guidance throughout this research.

I would also like to thank my parents for giving me this opportunity and for their continuous love and support throughout my life.

I would also like to thank my committee members Dr. Patrick Phelan and Dr. Qiong Nian for willing to serve on the committee and for their feedback on the research.

TABLE OF CONTENTS

Page

CHAPTER Page

LIST OF TABLES

LIST OF FIGURES

Figure Page

LIST OF ABBREVIATIONS

Abbreviation		Meaning
1.	CL	Catalyst Layer
2.	DOE	Department of Energy (U.S.)
3.	EIA	Energy Information Administration
4.	EMF	Electromotive force
5.	FEP	Fluorinated ethylene propylene
6.	GDL	Gad Diffusion Layer
7.	HHV	Higher Heating Value
8.	IRENA	International Renewable Energy Agency
9.	LHV	Lower Heating value
10.	MPL	Microporous Layer
11.	Mtoe	Million Tons of Oil equivalent
12.	PEMFC	Proton exchange membrane fuel cell
13.	PTFE	Polytetrafluoroethylene
14.	PVDF	Polyvinylidene fluoride
15.	SDS	Sodium dodecyl sulfate
16.	SEM	Scanning Electrode Microscope

CHAPTER 1

INTRODUCTION

1.1 Why Fuel Cells

Global energy demand fell by 3.8% (150 Mtoe) in the first quarter of the year 2020 with up to 10% reductions in some regions, mainly due to the confinement measures taken to prevent the spread of Covid-19 [1]. Global coal (8%) and oil (5%) demand were hit the hardest mainly due to the reductions in electricity demand (-2.5%). However, there was an increase (about 1.5%) in the Renewable energy demand, due to the new wind and solar projects completed in past years. EIA predicted that carbon emissions are still going to increase till the year 2050 owing to the high economic growth scenario [2]. This strongly indicates the need to find more clean energy solutions to tackle climate change, especially in the transportation sector as internal combustion engines are the major contributors to global CO_2 emissions [1]. Renewable energy sources have the potential to overcome these challenges, and in this regard, sustainable hydrogen energy is seen as a promising solution, as it can reduce global greenhouse gas emissions [3], [4]. By 2050, hydrogen will have about a 6% share in the global energy consumption as predicted by IRENA, whereas the hydrogen council suggests that a share of around 18% is possible because hydrogen can be produced from a variety of sources that are in abundance on earth [5]. By combining electricity and hydrogen we may be able to form a permanent system known as a "hydricity economy" which will be able to satisfy all future energy needs [6].

Among all the available alternatives fuel cells can be used for a variety of applications including transportation, stationary batteries (using Solid Oxide Fuel cell technology), the proton exchange membrane Fuel cells (PEMFC) can be a suitable candidate to replace

conventional power systems because of their high power density and environmental compatibility with transport applications [7]. Some other advantages of fuel cells include low cost, efficiency, less complex, environment-friendly, silent operation [8].

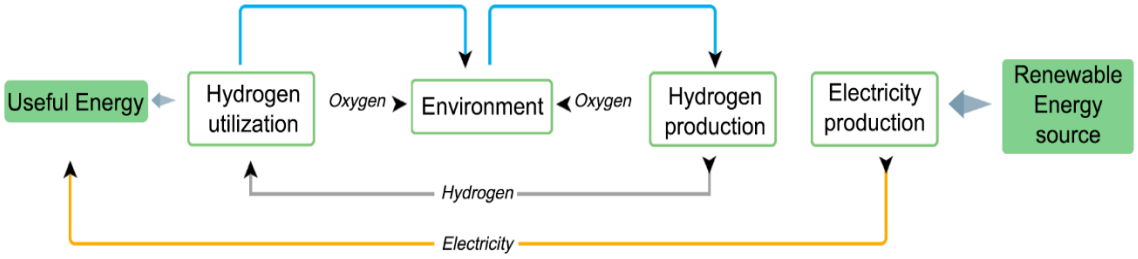

Fig. 1 – A sustainable model of Hydricity economy

1.2 Fuel cell Principles

The first fuel cell demonstration was done by scientist Sir William Grove in 1839, which used the basic principle of electrolysis of water. It was called the Gas Voltaic Battery by sir W.R. Grove, but the working principle was the same as a Fuel cell. The water was separated into hydrogen and oxygen when an electric current was passed through it, and when the electrolysis is reversed – hydrogen and oxygen combine to produce an electric current [9].

However, the basic reactions in the PEMFC are the same as the acid-based fuel cell developed by Sir Grove in 1839. The principal reaction undergoing the fuel cell is:

$$2H_2 + O_2 \rightarrow 2H_2O \qquad [1.1]$$

And electrical energy is generated in the reaction. Hence, a Fuel Cell is an electrochemical device that converts chemical energy into electrical energy, and the output is direct current (DC) [10]. However, the individual reactions taking place at the electrodes of the fuel cell are:

At Anode, hydrogen ionizes into proton and electrons,

$$2H_2 \rightarrow 4H^+ + 4e^- \quad [1.2]$$

At Cathode, the oxygen reacts with hydrogen to produce water,

$$O_2 + 4H^+ + 4e^- \rightarrow 2H_2O \quad [1.3]$$

Which is equivalent to

$$\frac{1}{2}O_2 + 2H^+ + 2e^- \rightarrow H_2O \quad [1.4]$$

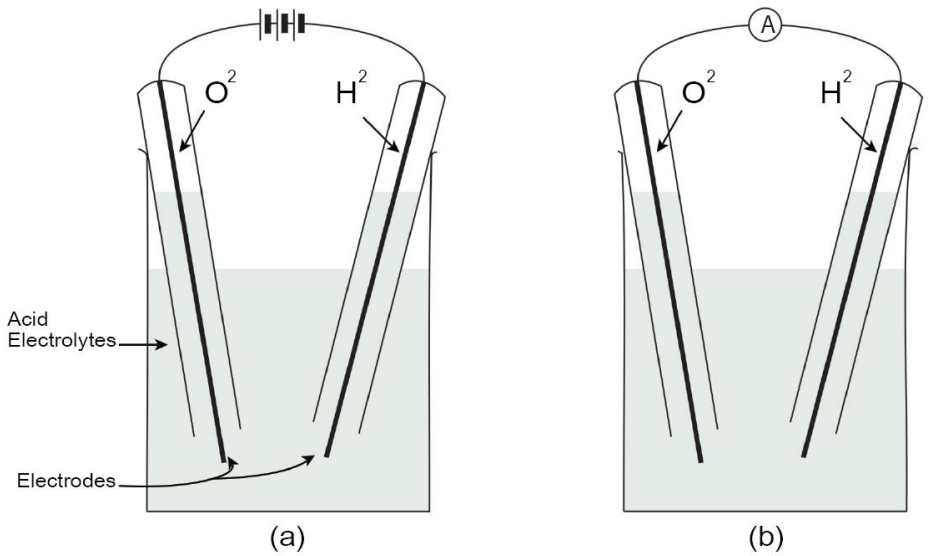

Fig. 2 – (a) Hydrogen and oxygen are separated when an electric current is passed through the electrolyte. (b) Recombining hydrogen and oxygen produces an electric current

This makes it clear that the electrons travel via an external circuit from the anode side to the cathode and on the other hand, the protons get transferred through the electrolyte, whose primary responsibility is to make sure that only protons are transferred through it [9]. Research has allowed using certain polymers as an electrolyte which are known as Polymer electrolyte membranes or proton exchange membranes [11].

The key components of the PEM fuel cell are membrane, Catalyst layer, gas diffusion layers, electrodes, and bipolar plates, however, the main focus of the thesis is the

performance and the durability of different gas diffusion layers with and without the pore-forming agent, which will be discussed in further chapters.

There were 2 sets of experiments conducted during the research mentioned in the thesis. The first was to evaluate the best composition of the PUREBLACK® based GDLs with and without PEG, and a comparison was made to the commercial GDL (AvCarb GDS 2120) to assess the feasibility of the research. It is worth mentioning that the MEAs with GDLs containing a single layer exhibited ~450 and ~1350 mW cm^{-2} in H_2/Air and H_2/O_2, respectively both at 60 and 100% RH conditions See figure 1.

Table 1. Configuration of the GDL samples for phase-1.

Sample ID	MPL sublayer	PEG (wt. %)
1	1	0
2	1	30
3	4	0,10,20,30
Commercial	1	-

Table 2. GDL samples for phase – 2 according to the time interval

GDL	Method	Time intervals			
PUREBLACK® (PB)	H_2O_2	PB0	PB8	PB16	PB 24
	H_2O	PB250	PB500	PB750	PB1000
VULCAN® (VL)	H_2O_2	VL0	VL8	VL16	VL24
	H_2O	VL250	VL500	VL750	VL1000
Commercial (COM)	H_2O_2	COM0	COM8	COM16	COM24
	H_2O	COM250	COM500	COM750	COM1000

The second phase of the study focused on the accelerated stress tests to access the durability of the PUREBLACK® based GDLs along with the VULCAN® (XC72R) carbon-

based GDLs while keeping all the other constituents (pore-forming agent, catalyst, membrane, etc) same. Only one composition (using 30% PEG) with repetitions for each of the GDLs were tested and a comparison was made with the commercial GDL.

1.3 POLYMER ELECTROLYTE MEMBRANE FUEL CELLS

The first Polymer electrolyte membrane fuel cell was developed by General Electric in the early 1960s, which was used in the U.S. Space Gemini program [12]. These fuel cells used solid Sulfonated polystyrene membranes functioning as the electrolyte, which were later replaced by Nafion® membranes made by Dupont in 1966 [10], [12].

Nafion is the commercial name for the copolymer sulfonated tetrafluoroethylene and its structure is given in figure 3. Nafion is considered the 'industry standard' and is made by substituting fluorine for hydrogen in the polyethylene polymer. Then a side chain of sulphonic acid is added, this process is called Sulphonation.

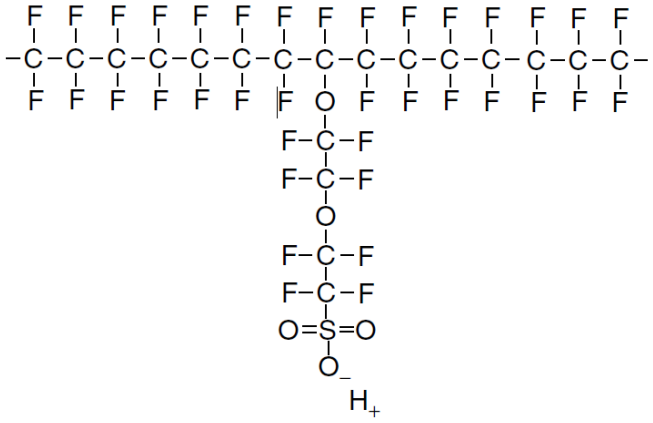

Fig. 3. One of the possible structures of Nafion or sulfonated fluoroethylene

1.3.1 Membrane

The key component of the PEMFC is the Polymer membrane which works as the electrolyte allowing the conduction of only protons from the anode side to the cathode and is also impermeable to gases. Therefore, it is often referred to as the Proton exchange

membrane. This membrane is sandwiched between two electrodes as shown in figure 4. usually made of carbon cloth or carbon fiber paper, which are porous and conducts electricity. This arrangement is known as the membrane electrode assembly (MEA) as shown in figure 4, which is usually connected in series using bipolar plates known as the stack to create the practical potential required. Nafion membrane (membrane NR-211) from Ion Power was used for all the samples in this study.

Fig. 4 – Membrane electrode assembly

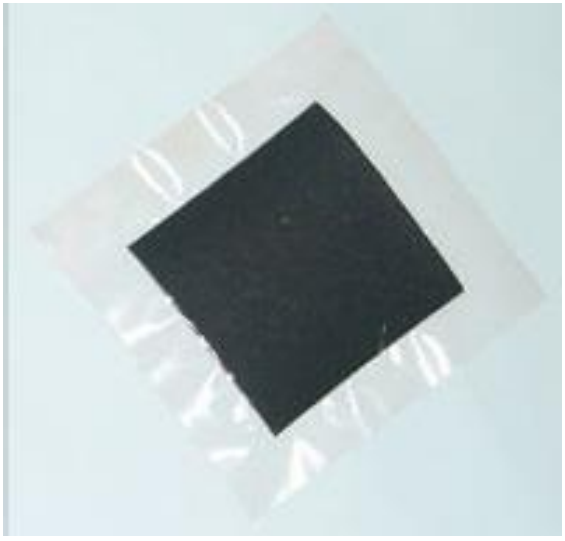

1.3.2 Catalyst

A catalyst (typically platinum) is needed to break the diatomic bond of the diatomic gases at both the cathode and anode sides, this catalyst is formed into very small particles on the surface of larger particles of finely divided carbon powders, and hence the layer formed is known as the Catalyst layer (CL). The CL is between the porous electrode and the polymer membrane and hence the CL is defined as the region where the electrochemical reactions take place [11].

The catalyst particles are joined to the electrolyte on one side and the gas diffusion layer (GDL) on the other side. Also, a thin layer of electrolyte is in contact with the catalyst

to promote the three-phase contact between electrolyte, catalyst, and the reactant gas to increase the performance of the MEA. Many types of research focus on new materials for the catalyst or improving the efficiency of the already existing catalysts. However, this study used the same catalyst for all the samples and focused on the effect of the GDLs on the fuel cell performance.

1.3.3 Gas Diffusion Layers

In PEM Fuel Cells the layer between the catalyst layer and the bipolar plates is called the gas diffusion layer, electrode substrate, or diffusor/current collector [10], and the reactant gases hydrogen, and air/oxygen, flow to the catalyst layers from the flow channels through the GDLs. GDL also maintains the smooth transfer of gas and liquid water within the fuel cell [13], [14]. Some other important functions of GDL include: establishes an electrical connection between the catalyst layer and bipolar plates, heat removal from the catalyst layer to the bipolar plate, prevents sagging of MEA by providing mechanical support. Hence the GDL should have these required properties: Sufficiently porous, the proton conductivity is directly proportional to the water content, but excess water might block the pores in the electrolyte or the GDL and can cause flooding [8], electrically and thermally conductive, pores facing CL must not be too big and it must be rigid enough to support the MEA with optimum bending stiffness, crack-free surface morphology, durability at various operating conditions [10], [15], [16].

Independent properties like water management, porosity, and graded structure of GDL have a strong effect on the performance of the PEMFC. Pore structures influence the flow of water droplets as explained by Kannan et al., which concludes that water flows with fewer restrictions in the concave and hydrophilic pore [17].

1.3.4 Substrates

The gas diffusion media also knows as the microporous substrates are generally made of either carbon fiber materials such as carbon fiber paper or woven carbon fabrics mainly because they can work in an acidic environment, have high gas permeability and electron conductivity, and is elastic on compression [18].

To enhance the mechanical strength and electron conductivity of the carbon fibers graphitization at high temperatures (>2000 ℃) is done. These carbon fibers are usually impregnated with a thermoset resin, on the other hand, spinning and weaving are incorporated to produce carbon cloths, then they are subjected to carbonization or graphitization [19], [20].

The substrate used was a non-woven, teflonized carbon paper (GD07508G) & (GD07508T) from Hollingsworth & Vose Company, USA, for phase -1 and phase – 2 respectively.

1.3.5 Hydrophobic and hydrophilic Treatments

The water management in the Gas diffusion media is usually maintained by hydrophobic treatments. Several hydrophobic agents have been implemented including, Polytetrafluoroethylene (PTFE), fluorinated ethylene propylene (FEP), and polyvinylidene fluoride (PVDF) [21]–[23].

But, substrates are usually treated with PTFE to avoid flooding, this is done by making it hydrophobic at both the anode and cathode sides. The PTFE loading generally ranges from (5% to 30%) and is usually applied by dipping the substrate in the PTFE solution, then drying and sintering at high temperatures [10]. Gas and water transport could be improved by adding PTFE, but excessive PTFE content could lead to a high flooding level in the

catalyst layer, hence an optimized PTFE content is required for the best performance of the MEA [24], [25].

The GDLs are strongly reliant on the microporous substrate and there is a strong link between gas permeability and distribution of pore size along with water management and hydrophobic pores. Liquid water is formed at the interface between the cathode catalyst layer and the microporous layer (MPL) during the activity of the fuel cell. The liquid water can easily transfer (or transport) to the flow field channels, primarily through the larger pores of the MPL and the carbon substrate [26], [27]. Owing to their hydrophobic properties, the smaller pores of the microporous layer (MPL) restricts liquid water and serve as routes for the transport of reactant gases to the reaction region [28]. The remaining water is pushed to the anode side through the membrane due to the insufficient capillary pressure needed for the water to reach the smaller pores, leading to reduced flooding of the GDL and the catalyst layer and improved membrane hydration [29].

A highly conducting porous carbon slurry along with a hydrophobic binder was used to fabricate the MPL on the GDL layer [13]. In the early stages, PUREBLACK® carbon was used as conducting matrix in lithium-ion battery [30] and was later introduced by Kannan et al. for the development of the MPL of the GDL, due to its partly graphitized core-shell property, this carbon had uniform as well as graded porosities [31], [32].
According to the following equation,

$$D_{eff} = \frac{\varepsilon}{\tau D} \qquad [2.1]$$

Where ε is the porosity, D is the binary diffusion coefficient of oxygen in nitrogen, and τ is the tortuosity, bulk porosity is expected to influence the effective diffusion coefficient (D_{eff}) of the porous media[33].

The porosity, ε, also depends on the compressed thickness:

$$\varepsilon = 1 - \frac{W_A}{\rho_{real} d} \quad [2.2]$$

where W_A is the weight per unit area, d is the thickness, and ρ_{real} is the solid phase density[10].

Gas diffusion media including GDL are made typically of multi-layered carbon porous materials that are by definition porous. GDLs are usually porous materials based on multi-layered carbon. Having a macro-porous substrate or backing provides the gas reactants and the water product with mechanical power, electrical conductivity, and mass transport, and they also contain at least one microporous layer that enhances electrical conductivity and water management. The pore size of the macro-porous substrates is much larger than the catalyst layers' average pore size [17]. Mercury porosimetry or immersion method can be used to measure the bulk porosity of the GDL.

1.3.6 Surface morphology and structure

The capillary law explains the relationship between pore diameter u_p and the applied pressure p, assuming that all pores are cylindrical.

$$d_p = \frac{4\gamma Cos\theta}{p} \quad [2.3]$$

Where γ = surface tension, θ = contact angle with the microporous layer. In the micro-porous layer, the micro-porous channels have a strong capillary force to absorb the gas input and water output [17].

The structure and the surface morphology of the GDL can be used to determine its functionality. The pore size structure and the gradient of pore sizes from the macro-layer to the micro-layer can be revealed by the microscopic view of the cross-section of the

GDLs. Several treatments have been documented to bring about structural modifications to the GDL and impart the necessary balance of hydrophilicity and hydrophobicity. The macro-porous gas diffusion backing and micro-porous layer are usually found in the GDL layers. On one side or two sides of the GDL, the micro-porous coating consisting of carbon black powder and a hydrophobic agent is used. In GDL, this layer is the main part to improve the efficiency of the fuel cell as it functions both as a valve that moves water away from the GDL to the flow field to minimize water flooding and transports the input gas into the catalyst layer from the flow field.

1.3.7 Fuel Cell Performance

'Gibbs free energy' – defined as the energy available to do external work, is the most important 'chemical energy' in the fuel cell. The movement of electrons around the external circuit is referred to as the 'external work' in a fuel cell. Equation 1.4 depicts that for each molecule of hydrogen used and for each molecule of water produced, two electrons must pass through the external circuit. Therefore, for each mole of Hydrogen $2N$ (N Avogadro's number) electrons are used. Hence, the Gibbs free energy released will be equal to the electrical work, if the system is reversible or is loss-free. And, the fundamental equation of the electromotive force (EMF) or the open-circuit voltage of the Fuel cell can be given by:

$$E = \frac{-\Delta \overline{g_f}}{2F} \qquad [2.4]$$

Where E = electromotive force, $-\Delta\overline{g_f}$ = Gibbs free energy, F = Faraday constant. The voltages that can be obtained if the system was 100 % efficient would be, 1.48 (using the HHV) and 1.25 (using the LHV). However, in practice, the voltage is usually low as some fuel has to pass unreacted [8].

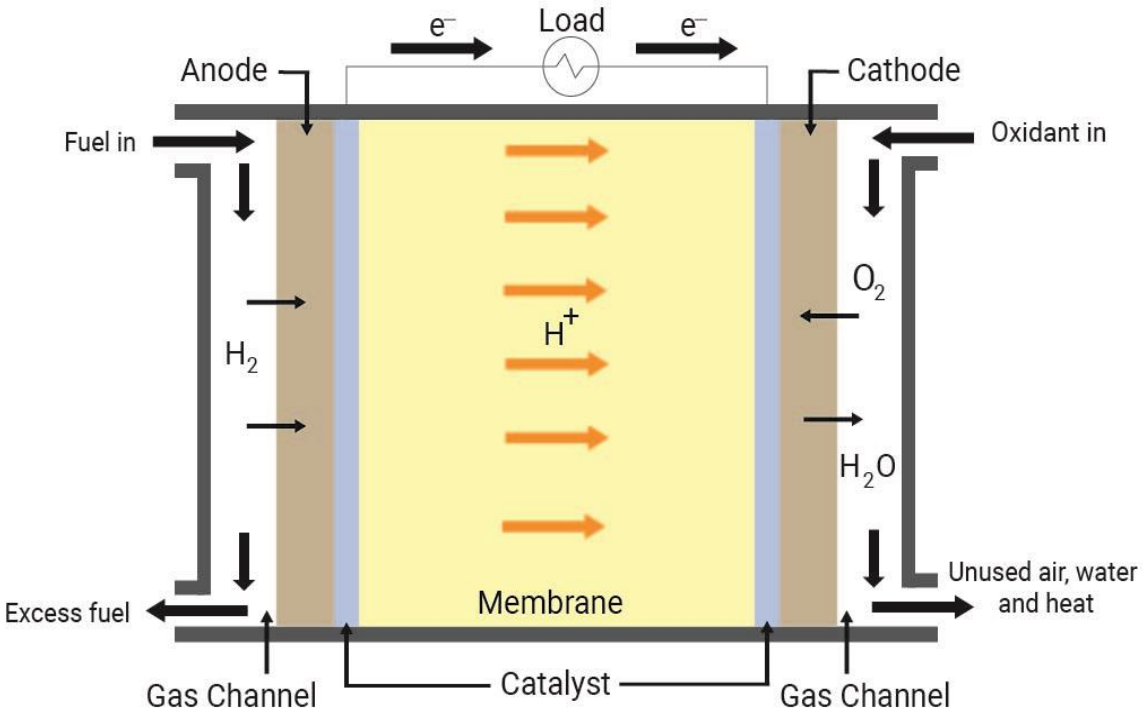

Fig. 5 – A single cell configuration of PEMFC and its working mechanism

1.3.7.1 Voltage Losses

Even when no external current is generated, the *open-circuit voltage* is significantly lower than the theoretical voltage. It goes below 1 V in most cases, which clearly illustrates the presence of losses in the fuel cell system. The factors influencing the voltage losses are as follows:

- The internal resistance of the circuit, electrical or ionic
- Stray currents
- Transmission losses in carrying reactants to reaction sites

- Electrochemical reactions kinetics
- Reactant crossover

In electrochemistry language, terms like polarization or overpotential are usually used instead of voltage losses, although the same physical meaning of these terms is the same [8].

1.3.7.2 Activation Polarisation

Due to the slow electrode kinetics, starting the electrochemical reaction from equilibrium requires some voltage difference. This electrochemical process caused by an overpotential introduced during current flow through the electrochemical cell to move an electrochemical cell from its equilibrium state is called Activation polarization [8], [34]. Activation polarization losses are usually lower when the exchange current density is higher. There are other losses including, Internal currents, crossover losses, ohmic losses, and concentration polarization, but are not discussed in depth in this study. The effect of each loss if present is mentioned in the further sections. If we subtract all the losses (activation polarization, ohmic, concentration polarization losses) from the equilibrium potential, we will get the polarization curve which is given in figure 6. These curves are the most important characteristic to measure fuel cell performance. These curves are used for the diagnostic, sizing, and controlling of fuel cells.

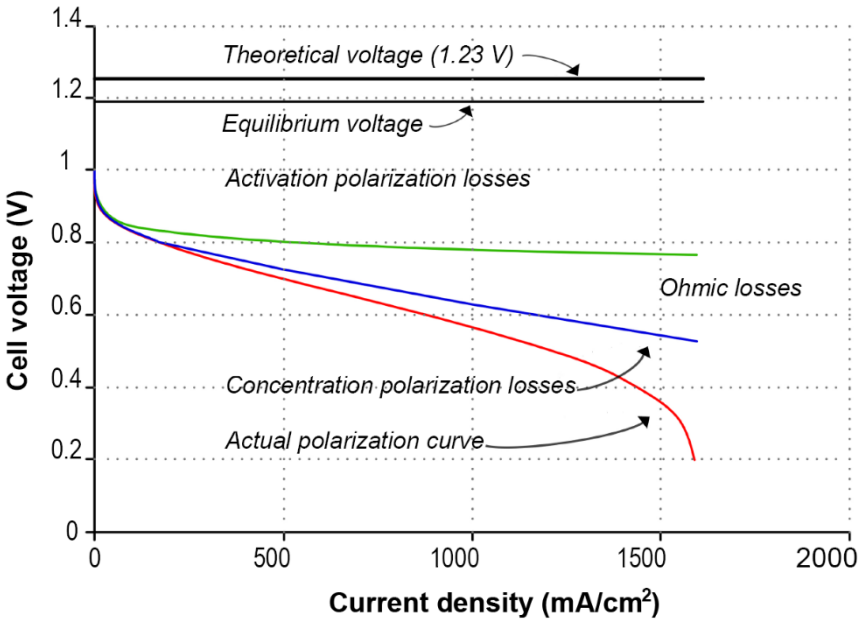

Fig.6 – Voltage Losses in Fuel cell

1.3.8 Durability

Certain lifetime conditions for high-temperature PEMFC have to be satisfied to enable the commercial use of these technologies in transport as well as stationary conditions, and that is still a developmental challenge for some of its applications. Under realistic operating conditions, DOE targets the operation of 40,000 hours and 5,000 hours for stationary and transportation fuel cells, respectively. The conditions that may result in stresses on the chemical and mechanical stability of the fuel cell materials, components, and interfaces, like fuel impurities, starting and stopping, freezing and thawing, and humidity and load cycles, can be considered under realistic operating conditions [35].

Catalyst layer degradation has been the main focus of the degradation studies for some time [36], [37], but recent studies show that the degradation of the GDLs also has a significant impact on the Fuel cell performance [38]. GDL degradation can be characterized in two main categories, mechanical and chemical degradation as given in figure 7. Any physical breakdown of the GDL can be classified as mechanical degradation whereas carbon corrosion is the main factor for chemical degradation, this might be due to the structural breakdown during conditions like local fuel starvation, start-up, and shut-down, where the water washes away the carbon [39], [40]. A decrease in hydrophobicity and the increase in the mass transport resistance were the major outcomes of the GDL degradation as reported in some studies [36]–[38], [41]–[43].

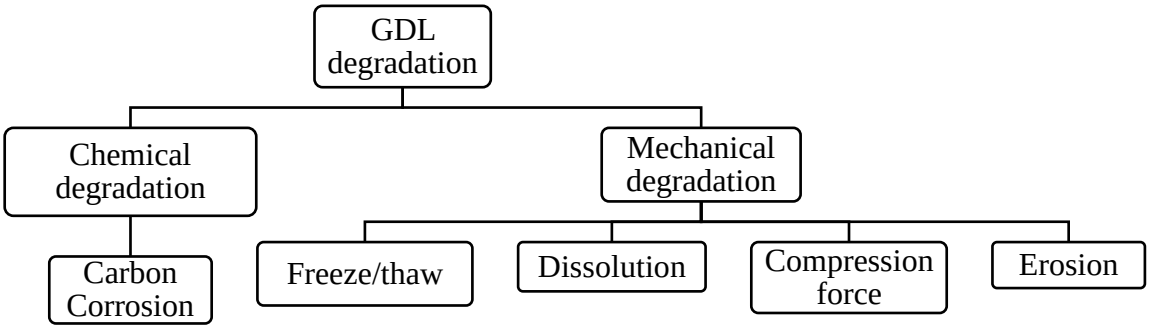

Fig.7 – Degradation mechanisms of GDLs

According to the first *fuel cell law*, which states that at least two parameters undergo a change if one parameter of the fuel cell is changed, and hence one cannot just change only one parameter of a fuel cell. Therefore it becomes necessary to isolate the degradation of the GDL, in this regard some ex-situ methods have been developed and performed where a loss in hydrophobicity was observed [42], [44], [45]. A comprehensive study by J Park et al. reviews the durability and degradation of the GDLs in the PEMFC [40].

For phase-2 of the study, the dissolution effect on GDL was used to conduct the Accelerated stress tests.

1.3.8.1 Dissolution effect on GDLs

As mentioned in earlier chapters, water is produced in the fuel cell during the electrochemical reaction when oxygen and hydrogen react. This exposes the GDL to water or an oxidative environment, and the water can get accumulated onto the GDL. This causes the degradation of the carbon material of the GDL as it gets dissolved and produces oxides, hydroxide, and other species [46], [47].

H_2O_2 is produced when two-electron reduction occurs on the platinum catalyst [48].

$$O_2 + 2e^- + 2H^+ \leftrightarrow H_2O_2 \ (E_0 = 0.695\ V_{RHE})$$

On the other hand, carbon dioxide is produced after the complete oxidation of elemental carbon by water [49].

$$C + 2H_2O \rightarrow CO_2 + 4H^+ + 4E^- \ (E_0 = 0.207\ V_{RHE})$$

1.3.8.2 Accelerated Stress test

Bosomoiu et al. [38] performed the degradation study of the GDL hydrophobicity for 1000 hours of operation which was one of the longest recorded studies under in-situ conditions. This shows the huge amount of time and resources utilized in the research and hence presents a need to find the solutions in terms of accelerated degradation mechanisms [50].

Several protocols like freeze/thaw cycling and others, which focuses on mechanical degradation of the GDL have been developed for the in-situ accelerated degradation of the GDLs in the literature [51], [52] along with the protocols established by the DOE and the

Fuel Cell Technical Team of the US Drive who have developed the ex-situ and in-situ component-level accelerated stress tests [35], [53].

In this study two different methods for the ex-situ ageing of the GDLs were implemented, one was to age the GDL samples in 30% Hydrogen peroxide (H_2O_2) solution at 90 ℃ for 24 hours [54], and the second approach was to age the GDL samples by immersion in water at 80 ℃ for 1000 hours [55]. A comparison between the durability of the PUREBLACK® based GDLs and VULCAN® (XC72R) carbon-based GDL alongside a commercial GDL was made.

CHAPTER 2

METHODOLOGY

2.1 Pore Size distribution

The total pore volume can be measured using the mercury pore size analyzer by calculating the amount of mercury penetrating the pores of the GDL as a function of the pressure applied. The pressure required depends upon the diameter of the pores [17]. PoreMaster-60 Automatic Mercury Intrusion Analyser by Quantachrome Tech, Florida was used to measure the pore size distribution of the GDL samples under low and high-pressure modes.

Pore size measurement from over 1100 (at contact angle 150) micron to 0.0036 microns in pore diameter is possible with the PoreMaster 60 porosimeter, which generates pressure up to 60,000 psia.

2.2 Surface Morphology of GDLs

XL-30 Environmental FEG (FEI) Scanning Electrode Microscope (XL30ESEM-FEG) was used to investigate the surface morphology and cross-section of the GDL samples. At pressures as high as 10 Torr and sample temperatures as high as 1,000°C, the XL30 SEM-FEG provides high-resolution secondary electron imaging. For observation of samples in conventional high vacuum SEMs, the XL30 FEG-SEM uses a stable, high brightness Schottky Field Emission Source.

An electron probe with a diameter of 2-50 nm is focused on the specimen in scanning electron microscopy (SEM). A scan generator rasters this concentrated beam across the sample while also driving the image monitor's x- and y-scan coils. Then a 2-D map of the

near-surface topology, composition, and possibly electronic nature can be build by using the monitor intensity which is modulated by these signals.

2.3 Contact Angle

The contact angle is the angle created at the point where water, air, and solid meet, and its value indicates the probability of the surface being wetted by the water. Sessile-drop goniometry (Kruss Simple Drop) was used to examine the surface-wetting characteristics of the GDLs. A mixture of IPA-water (30:70) was used to evaluate the hydrophobic and hydrophilic properties of the surface of the PUREBLACK® and VULCAN® (XC72R) based GDLs with and without PEG along with the commercial GDL. The mixture was used keeping in mind the hydrophobic properties of the GDLs, mixing the water with IPA helps the droplets to stay longer on the surface of the GDLs.

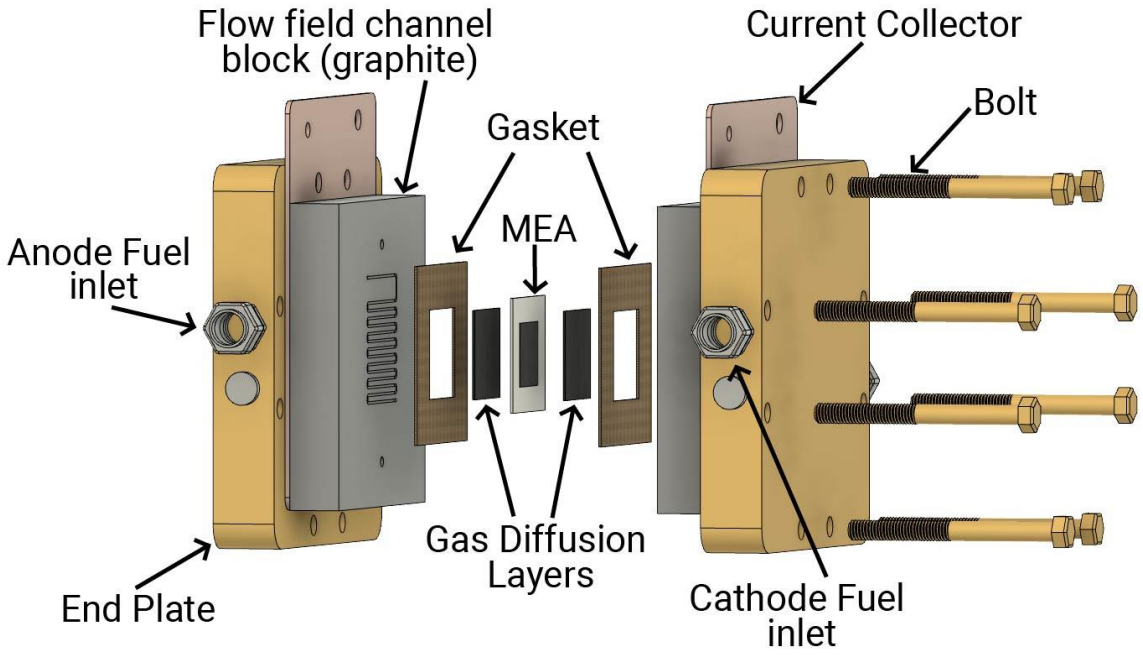

Fig.8 – CAD model for reference of the single-cell Fuel cell

2.4 Fuel Cell Performance

For the evaluation of the catalyst coated membranes (CCMs) and the GDL samples, a single cell fuel cell from Fuel Cell Technologies Inc, USA was used (Fig. 8). A uniform torque of 4.5 Nm was used along with the silicone coated fabric gaskets (Product # CF1007, Saint-Gobain Performance Plastics, USA) for the gas sealing of the fuel cell. The industry-standard testing station (Figure 9) from Greenlight (G40, Hydrogenics, Canada) was used to evaluate the performance of the fuel cell at 70 °C.

Fig. 9 – Fuel cell testing station (G40, Hydrogenics, Canada)

CHAPTER 3

EXPERIMENTAL

In this study, Pt catalyst (TEC10E50E, 46% Pt on carbon, Tanaka) ink in isopropyl alcohol (15 mL for 1 g of catalyst) was used to fabricate the Catalyst Coated Membranes (CCMs). The ink also contained 1.2 mL of Nafion dispersion (LIQUION LQ-1105, 5 wt % Ion Power, Inc.,) [56]. The geometrically active area of the Nafion membrane (Membrane NR-211) was 5 cm^2 which was sprayed with the catalyst ink using the micro-spray technique on both anode and cathode sides, which gave the uniform Pt loading of ~0.4 mg per cm^2.

In the first phase, GDLs were manufactured using PUREBLACK® carbon-based slurry to achieve graded and fixed porosity with and without a pore-forming agent in the MPL.

Nano-chain carbon powder PUREBLACK® 205-110, from Superior Graphite Co., Teflon Emulsion (PTFE DISP30) from Dupont, sodium dodecyl sulfate (SDS) from Acros Organics (CAS# 151-21-3) and polyethylene glycol (PEG-1500) from Aldrich Chemistry (CAS# 25322-68-3) were used for preparing slurry for fabricating the MPL. 0.5 g of PUREBLACK® carbon was dispersed in 80 mL isopropyl alcohol solution (Sigma-Aldrich, 99.7%, CAS# 67-63-0) containing 120 mg of SDS and various amounts of PEG (see Table 1), by sonication for 30 min, followed by stirring for 60 min. To achieve homogenous slurry, the Teflon emulsion (34 wt. %) was added dropwise into the mixture and stirred for 15 minutes. The carbon slurry was coated on a 10 x 10 cm^2 carbon paper substrate using the micro-spray technique. To achieve a uniform distribution of PTFE on carbon powder and thermal decomposition of PEG, the coated samples were dried

overnight at room temperature and sintered in air at 350 °C for 30 min. [57]. Later, to eliminate the SDS and the residual PEG, the samples were rinsed thoroughly in DI water. As mentioned above, the GDL samples in this study were fabricated with MPLs with and without PEG and the carbon loading was 3 ± 0.15 mg cm^{-2}, the configurations of the samples are given in Table 1. The same amount of carbon powder (~0.75 ± 0.04 mg cm^{-2}) was used for each layer and just the weight percent of PEG was varied to achieve the graded porosity for sample 3.

In the second phase, GDLs were manufactured using PUREBLACK® and VULCAN® (XC72R) carbon-based slurry with the pore-forming agent (30 % PEG) in the MPL. Several repetitions of the same composition of the GDLs were made for different testing and analysis.

VULCAN® (XC72R) (by Cabot Corporation, MA, USA) was used as the carbon powder, and other factors in the MEA were kept the same as Sample #3 form phase -1 which had the best performance. Accelerated stress tests were conducted using these GDLs and a fuel cell performance comparison between VULCAN® and PUREBLACK® based GDLs was made along with the commercial (AvCarb GDS 2120) based GDL. Quincy Lab 40GC Lab Oven was used to maintain the constant temperature of 80 ℃ for 1000 h and GDL samples (5 Nos. of 2.5 × 2.5 cm^2), immersed in deionized water, were placed. Then the samples were rinsed in DI water and dried at 80 ℃ overnight [44].

GDLs were submerged in 30 % H_2O_2 solution at 90 ℃ for 24 using the Heraeus UT12P Lab oven, this helps the accelerated degradation of the gas diffusion layer through carbon corrosion. Every 8 h the concentration of the hydrogen peroxide was measured using the manganometric redox titration with $KMnO_4$. Afterward, the samples were rinsed

and soaked in DI water for 12 h and dried at 80 ℃ overnight [58]. surface morphology, surface-wettability, and pore size distribution analysis were done for both the PUREBLACK® and VULCAN® GDLs before and after ASTs.

Galvanostatic polarization method at 60 % and 100 % RH using H_2/O_2 and H_2/air was used on the testing station while maintaining the flow rate of 200 SCCM at the anode and 300 SCCM at the cathode. The current was set at constant (600 $mA.cm^{-2}$) for durability testing at all conditions.

In phase - 1, the durability testing was done for only the PUREBLACK® based GDLs with and without 30 % PEG using H_2/Air at 60 and 100 % RH conditions.

For phase - 2, the durability testing was done for both the PUREBLACK® and VULCAN® (XC72R) based GDLs with 30 % PEG using H_2/Air at 60 and 100 % RH conditions

CHAPTER 4

RESULTS AND DISCUSSION

4.1 Phase – 1

4.1.1 Pore size distribution

Pore size distribution was measured to study the effect of the pore-forming agent on the performance of the fuel cell. The configuration of all the three different GDL samples used in phase – 1 is given in Table 1 and is represented in figure 10. The porosity gradient is from the flow fields to the catalyst layer of the MEA.

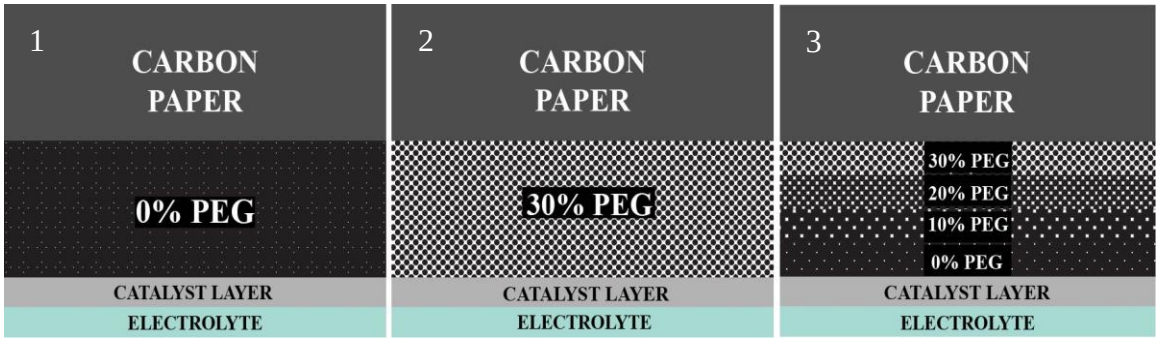

Figure 10 - Configuration of gas diffusion layer samples 1 - 3.

The comparison of the pore size distribution of the PUREBLACK® based GDLs with and without PEG is given in figure 11 and table 2.

Table 2. Total pore volume, contact angle, and porosity of all samples

Sample ID	Contact angle (Degrees)	Pore volume ($cc.g^{-1}$)	Low pressure pore diameter (µm)	High pressure pore diameter (nm)	Porosity
1	130 ± 2	1.48	47	90	~50
2	115 ± 2	1.72	44	90	~55
3	125 ± 2	1.23	43	90	~40
Commercial	87 ± 2	1.45	54	~300	~50

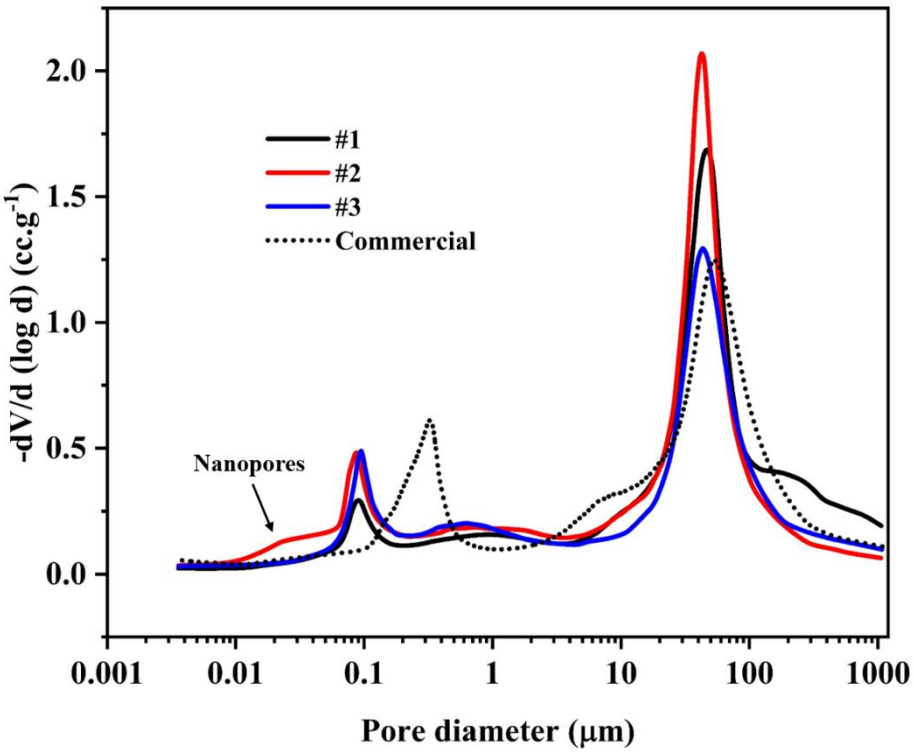

Fig. 11 - Pore size distribution for PUREBLACK® based GDLs (samples 1-3) along with commercial GDL (AvCarb GDS 2120), (Phase – 1).

The meso and micropores are represented by the high-pressure region below 1 mm and the macropores are represented by the low-pressure region above 1 mm, the micro/mesopores are responsible for the gas transfer while the macropores are responsible for expelling water [59]. Nanopores can be seen in the GDL with 30% PEG (Sample 2), this might help retain the electrolyte conductivity at lower RH conditions by keeping the product water at the catalyst layer and electrolyte reaction zone. Table 2 gives the total pore volume of all the samples, of which the total pore volume of sample 2 is the highest (1.72 $cc.g^{-1}$). Also, in the low-pressure area (macroporous carbon substrate), sample 2 displays the highest distribution of pore size, confirming its ability to efficiently water removal.

It is evident from Table 2 that increasing the PEG content significantly increased the pore size distribution in samples 2 and 3 as compared to the GDL without PEG

(sample1). This resulted in better gas transport to the reaction zone in samples 1 and 2. The commercial GDL, on the other hand, showed poor water transport characteristics at both low and high RH conditions, this can be attributed to its larger pore sizes in both regions, these larger pores might be due to the presence of surface cracks along with larger pores in MPL. Lobato J. et al. mentioned the presence of larger pore blockage of one MPL sublayer when the next sublayer was deposited can cause flooding at high RH conditions, this can be observed of the 4 sub-layered GDL with graded porosity (sample 3) with decreased pore size distribution [60].

4.1.2 Surface morphology of GDLs

The surface morphology of the PUREBLACK® based GDLs with and without PEG along with the commercial GDL sample is given in figure 12. Relatively smaller pores can be seen in sample 1 (single MPL sublayer without PEG), figure 12a, and sample 3 (four MPL sublayers with the top layer without PEG) figure 12b compared to sample 2 (single MPL sublayer with 30 % PEG) figure 12c. But larger mud-cracks on the surface are visible in multiple locations of the commercial GDL figure 12d. Some research reported reductions in electrical conductivity of the GDL with larger pores [61], but, efficient water removal that prevents flooding and uniform gas transport to the reaction zone can be achieved by the presence of a smooth, crack-free surface and homogenous nature of the MPL [62]. Water accumulation and forming defects around the cracks can take place due to the cracked surface of the commercial GDL, which can lead to rapid MPL degradation and can also lead to non-uniform reactant gases distribution and water removal which can also cause hot spots at the reaction zone [61], [63].

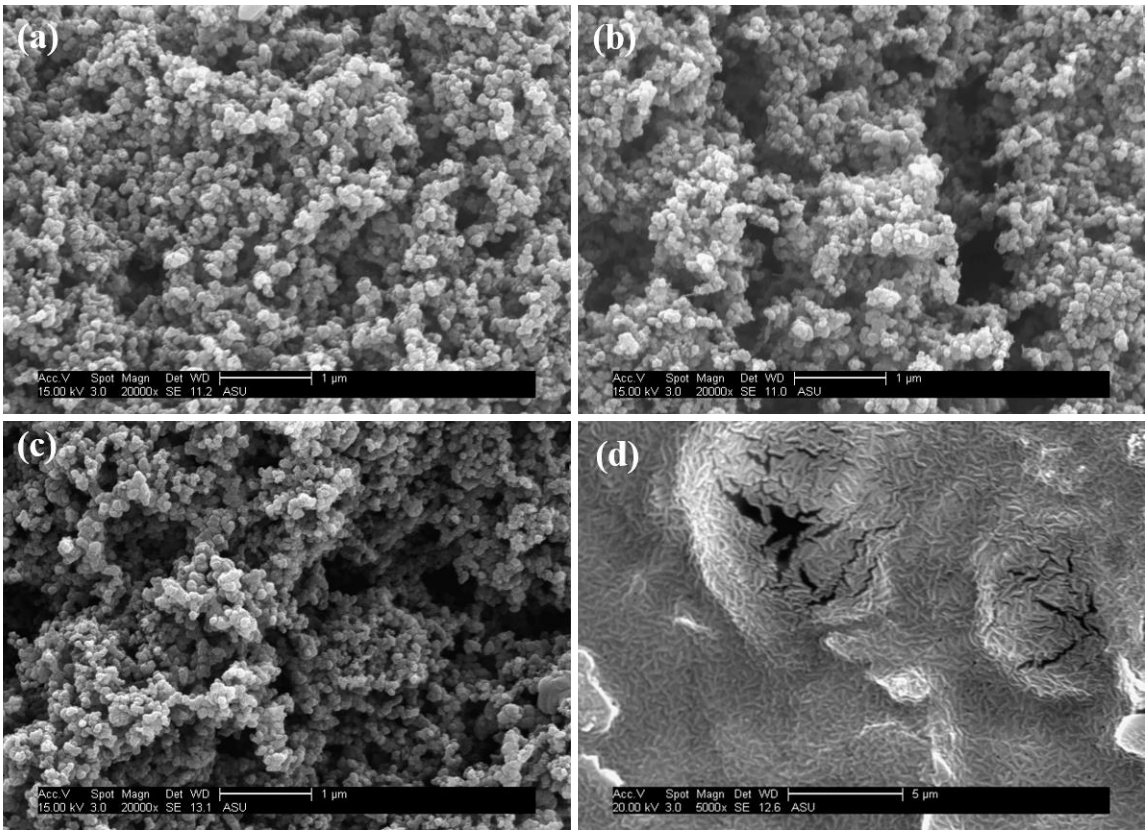

Fig. 12 - Scanning electron micrographs of (a) to (c) PUREBLACK® based GDLs (samples 1-3), and (d) commercial GDLs (AvCarb GDS 2120), Phase – 1.

To examine the bulk characteristics and the thickness of the GDLs, cross-section images were recorded PUREBLACK® based GDLs with and without PEG along with the commercial GDL sample (figure 12). Accurate measurement was difficult due to carbon bleed through the uncoated side of the macroporous substrate but as seen from Figure 13(a)-(c), the MPL thickness of the PUREBLACK® based GDLs ranges between 60-70 μm and the commercial GDL (Figure 13(d)) ranges between 25-30 μm. The commercial GDL is, therefore, more prone to flooding due to the relatively thinner MPL coating as the MPL provides a higher back-diffusion rate from the cathode to the anode through the membrane, reducing the liquid water saturation level in the catalyst layer [64].

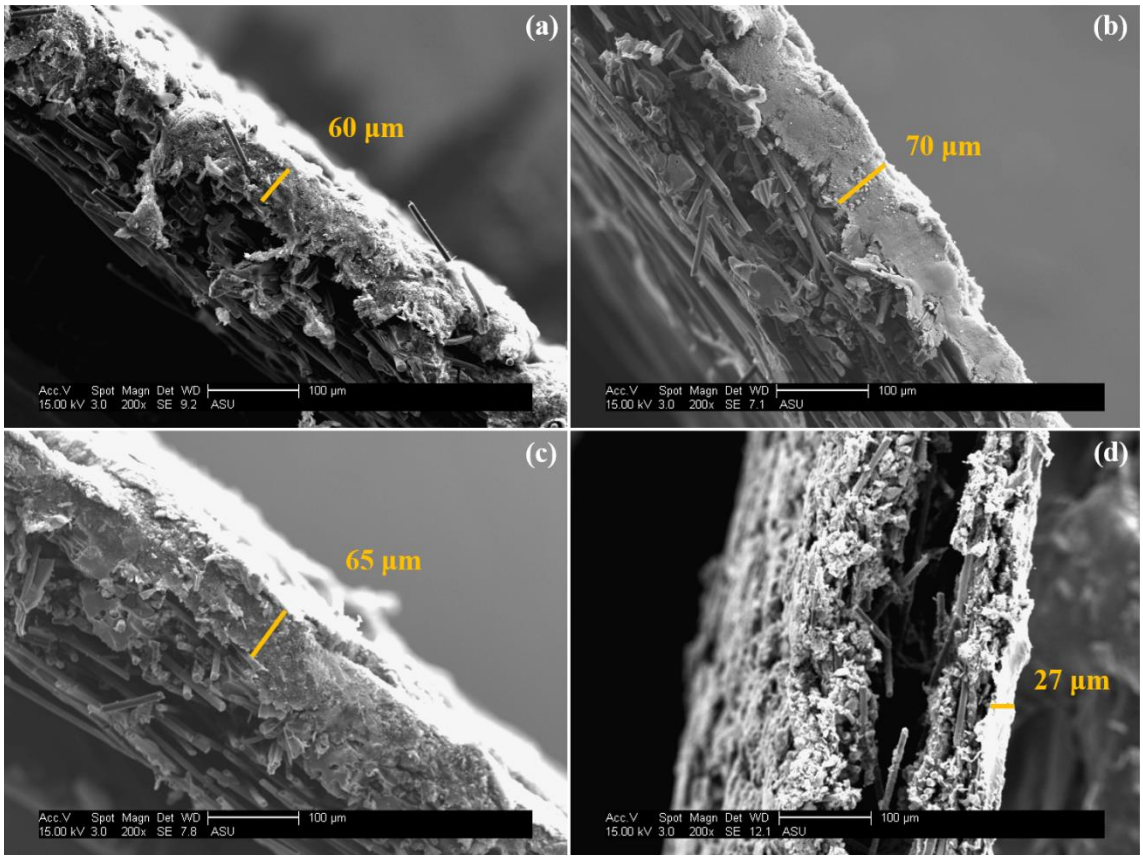

Fig. 13 - Scanning electron micrographs (cross-section) of (a) to (c) PUREBLACK® based GDLs (samples 1-3), and (d) commercial GDLs (AvCarb GDS 2120), Phase – 1.

4.1.3 Contact Angle

To examine the hydrophobic and hydrophilic characteristics of the GDLs with and without the pore-forming agent, the surface wettability was studied. In the first stage of the testing, the contact angle values for the PUREBLACK® based GDLs were well within the range of two degrees for 5 samples in each category of the GDLs tested (Table 2), and the values for the contact angle were 130°, 115°, and 125° for the PUREBLACK® based GDLs (fig 14(a-c)). Gas flow to the catalyst layer was expected to improve due to the relatively higher hydrophobic surface of the MPLs which expels the excess water efficiently [65]. Also, due to the higher porosity of the MPL of the GDL sample 2, a lower contact angle

was observed (fig 14(b)). On the other hand, a lower contact angle (87°) was observed in the commercial GDL which can lead to flooding and lower fuel cell performance at 100% RH condition [27].

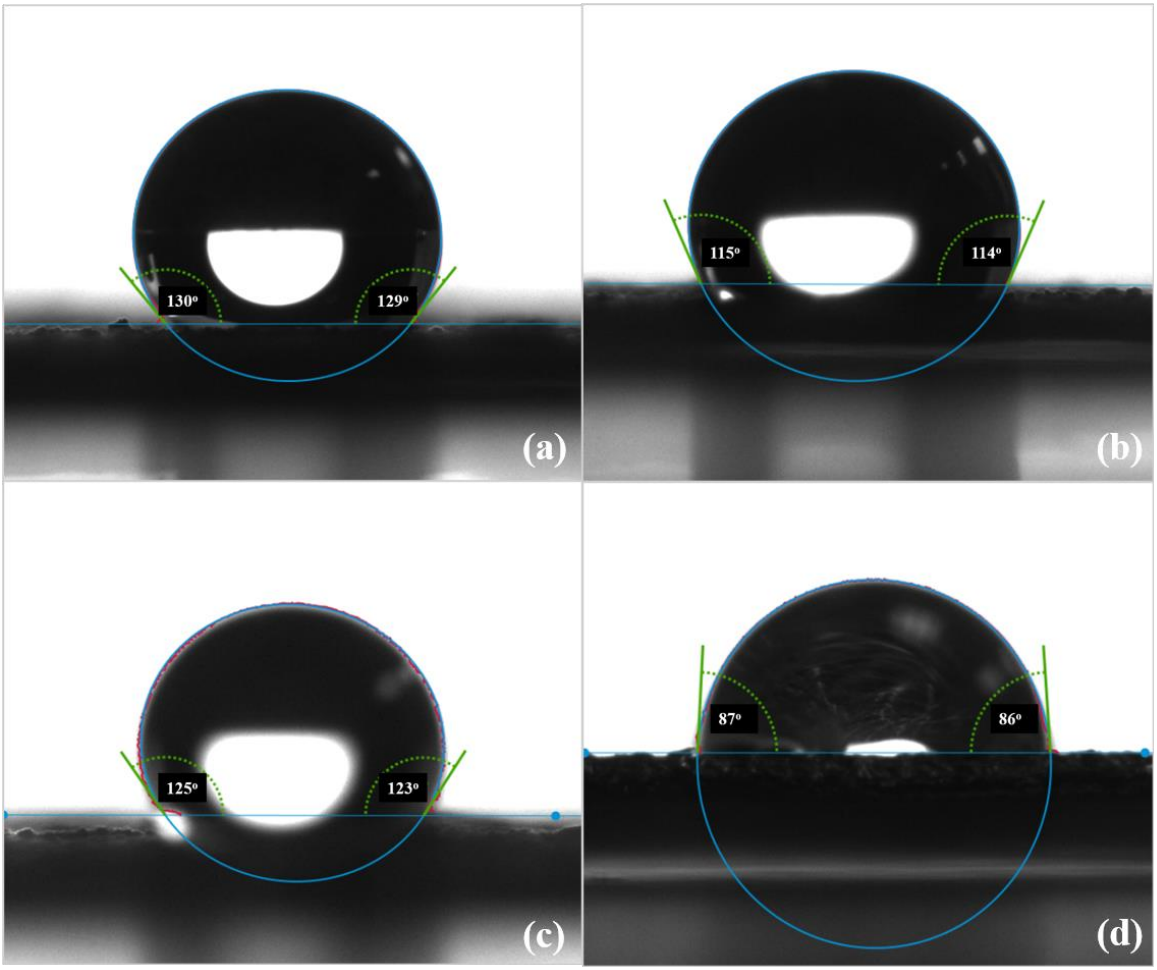

Fig. 14 – Contact angle images for (a) to (c) PUREBLACK® based GDLs (samples 1-3), and (d) commercial GDLs (AvCarb GDS 2120)

4.1.4 Fuel Cell Performance (Phase - 1)

Figure 15-16 shows the Fuel cell performance for all the GDL samples in phase – 1 including PUREBLACK® based samples and the commercial, at 70 °C using H_2/O_2 and H_2/air both at 60 % and 100 % RH conditions. The testing was done at 100 % RH first to

reduce the effect of membrane hydration, then the RH was dropped to 60 % at both the anode and cathode sides. The fuel cell performance using O_2 and air as oxidants at 60 and 100 % RH conditions for the PUREBLACK® based GDLs (sample 1) without a pore-forming agent is given in fig. 15(a) and 15(b).

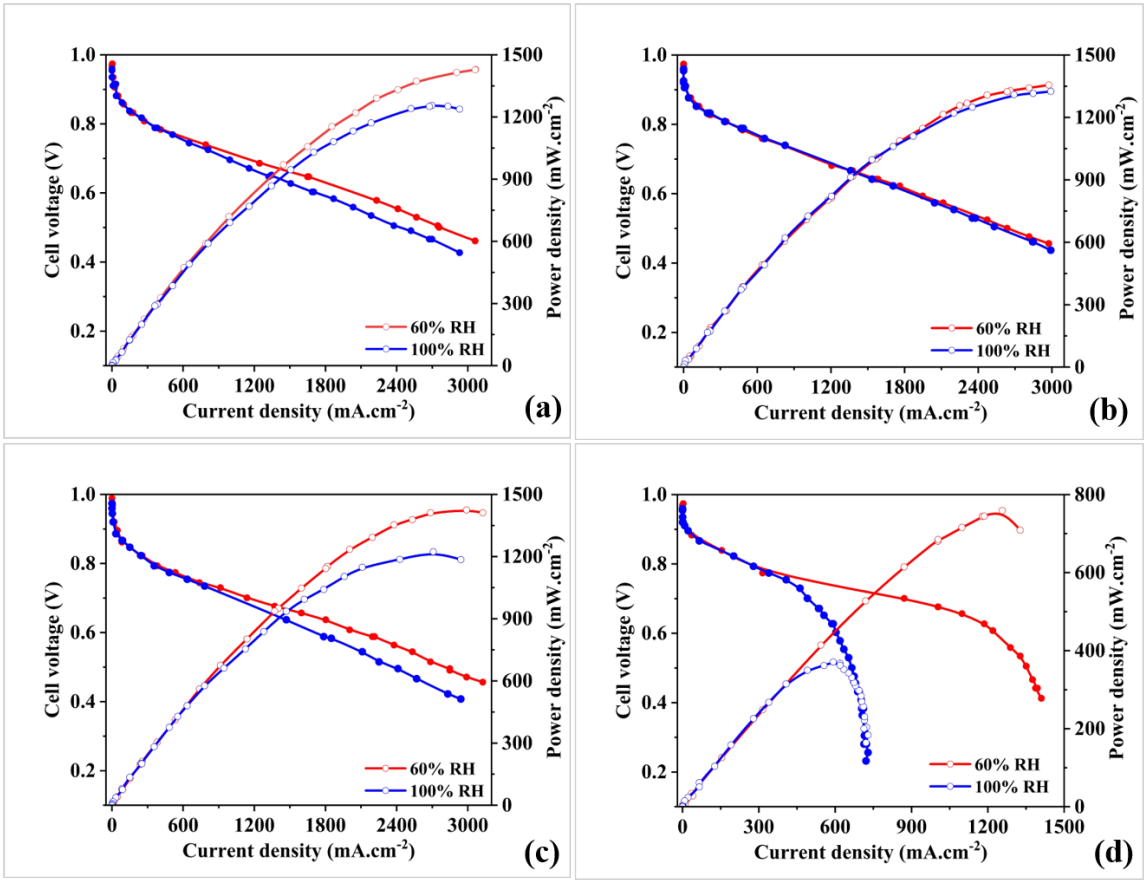

Fig. 15 - Fuel cell performance at 70 °C using H_2/O_2 at 60 and 100% RH for MEAs with (a) to (c) PUREBLACK® based GDLs (samples 1-3), and (d) commercial GDLs (AvCarb GDS 2120), Phase – 1.

The peak power density at 100% RH is much lower (1255 $mW.cm^{-2}$) compared to that at 60% RH (1430 $mW.cm^{-2}$) when using O_2 as the oxidant (fig. 15(a)). With air as the oxidant, the peak power density values of 436 and 397 mW.cm-2 at 60 and 100 % RH, respectively were observed which reflects the same trend as in O_2 (Fig. 16(a)). The reduced performance of GDL sample 1 without PEG can be attributed to the lower pore volume (see Figure 11),

due to which the MEA starts flooding at 100 % RH condition [66]. The fuel cell performance using PUREBLACK® based GDL with 30 % PEG as a pore-forming agent in the MPL using O_2 and air as oxidants is given in Figures 15(b) and 16(b), respectively. It can be noticed from fig 15(b) that the peak power density values while using O_2 as the oxidant were 1325 mW.cm^{-2} at 100 % RH and 1355 mW.cm^{-2} at 60 % RH. A similar performance trend is shown with air as oxidant (Fig 16(b)) with peak power density values of 444 and 432 mW.cm-^{2} at 60 and 100 % RH, respectively.

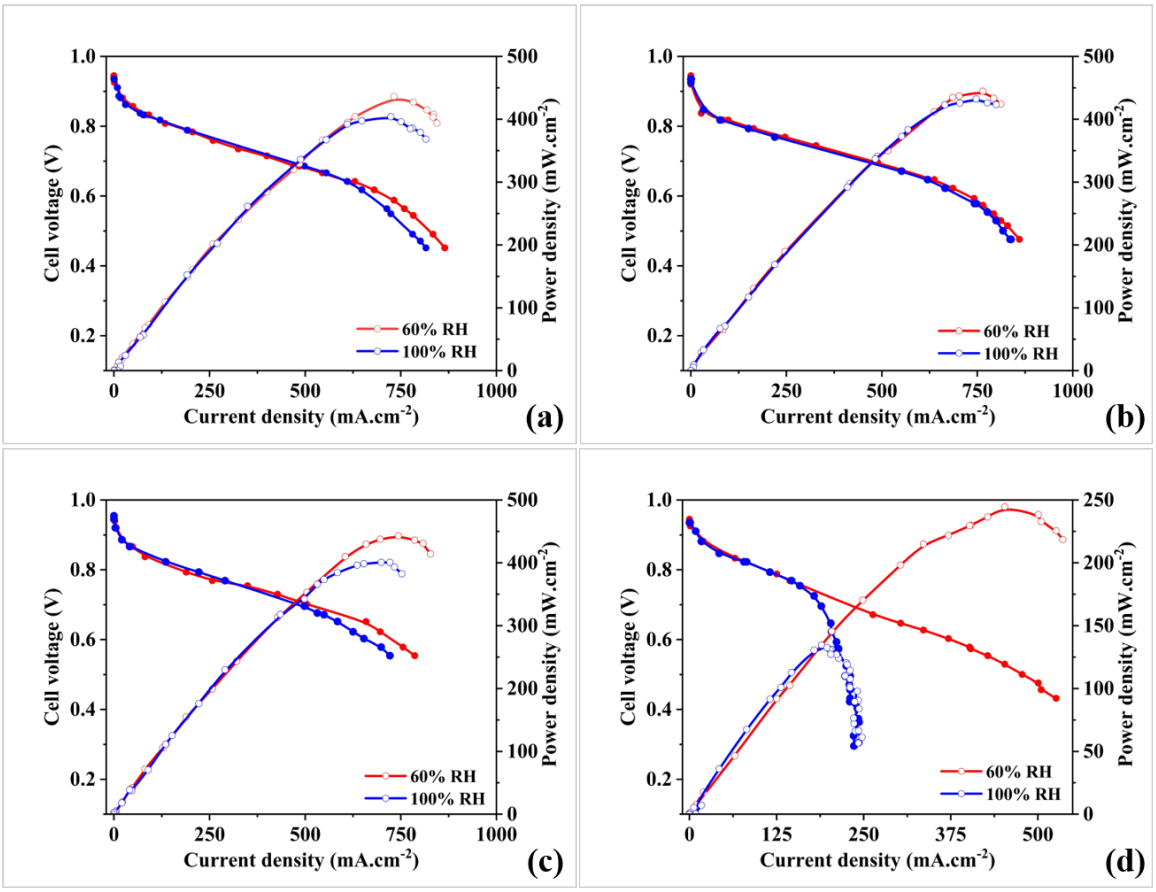

Fig. 16 - Fuel cell performance at 70 °C using H_2/air at 60 and 100% RH for MEAs with (a) to (c) PUREBLACK® based GDLs (samples 1-3), and (d) commercial GDLs (AvCarb GDS 2120), Phase – 1

The higher porosity (see Figure 11) could be the reason behind the higher fuel cell performance at both 60 and 100 % RH (using O_2 or air), as it prevents flooding by

facilitating better water transport, in particular at 100 % RH conditions [67]. MEA with GDL Sample 2 showed higher peak power density using air as oxidant at 60 % RH condition, this might be due to the presence of nanopores (Figure 11) that prevents the electrolyte from drying by retaining the product water [68].

The fuel cell performance using PUREBLACK® based GDL (sample 3) with graded porosity (0, 10, 20, 30% PEG) using O_2 and air as oxidants at 60 and 100 % RH conditions are given in Figure 15(c) and 16(c). The peak power densities for 60 and 100 % RH are 1425 and 1224 $mW.cm^{-2}$ with O_2 gas, and 442 and 400 $mW.cm^{-2}$ with air as oxidant gas, respectively which shows that the graded porosity did not have a significant effect on the fuel cell performance. The MPL carbon can block some of the larger pores created in each previous sublayer because the first MPL sublayer deposited on the carbon substrate has a greater amount of PEG and is followed by sublayers with a progressively reduced amount of PEG. Lower fuel cell performance is possible due to flooding that can happen in this configuration with a reduced number of macropores (Figure 11) as it inhibits efficient water transport at 100 % RH conditions [60]. For comparison purposes, the fuel cell performance for the MEAs with commercial GDL using O_2 and air as oxidants at 60 and 100 % RH conditions are given in Figures 15(d) and 16(d). The commercial samples exhibit very poor fuel cell performance with peak power densities of 761 at and 370 $mW.cm^{-2}$ at 100 % RH in H_2/O_2 and 258 at 60 % RH and 134 $mW.cm^{-2}$ at 100 % RH, in H_2/air. The poor performance of the commercial GDL sample can be attributed to its inability to efficiently transport water due to the presence of cracked surface morphology [61] (see figure 12) along with highly hydrophilic characteristics [27] (see Figure 14) of the microporous layer, and lower pore volume (see Figure 15) of the macroporous layer.

Lower fuel cell performance is also due to the presence of thinner MPL which reduces the membrane conductivity due to increased water saturation level in the GDL [69].

4.1.5 Durability

Owing to its high and stable performance at both RH conditions, the GDL with 30% PEG on the MPL (sample 1 and 2) were selected for the durability test using H_2/air as oxidant. Polarisation was performed before each RH change along with fully hydrating the system [70]. Before evaluating the performance stability at each RH condition, the fuel cell performance for the MEA with the GDLs (Fig. 17(c)) containing 30 % PEG using H_2/air at 60 and 100 % RH was conducted and is given in Figure 17(a). Fig. 17(b) and (d) show the cell voltage at 600 $mAcm^{-2}$ for 50 h at 100% RH first and then for 50 h at 60% RH conditions for the MEAs containing GDLs without and with 30% PEG, respectively. Overall, the performance of the fuel cell at 60 % RH remains identical (~400 $mAcm^{-2}$) after 50 h of continuous cell operation and has a negligible degradation at 100 % RH after 50 h of operation, which can be seen in Fig. 17(c). Figure 17a shows that the fuel cell performance is higher at 60 % RH condition, but there is a slight deflection in the voltage between 0.59 and 0.62 V after ~35 h of operation. This voltage is still higher in comparison to 100% RH, but the drop observed might be due to temporary O_2 starvation caused by flooding [71]. The voltage drops (to 0.58 V) at 100% RH are insignificant as the fuel cell performance is not governed by mass transport in this region. Resistance to corrosion during fuel cell operation was observed in the GDLs based on PUREBLACK® carbon with a well-defined graphitic structure [32], [72]. The assumption that under high current density a reduction in the O_2 transport to the reaction zone due to flooding is present under saturated conditions (100% RH), confirms the fuel cell improvement at 60 % RH after 10h

of operation [73]. The presence of nano-sized core-shell PUREBLACK® carbon-based microporous layer with 30% PEG increased the durability of the MEA as clearly seen from figure17(d) which shows a stable voltage of 0.58 V both at 60 and 100% RH conditions [74], [75].

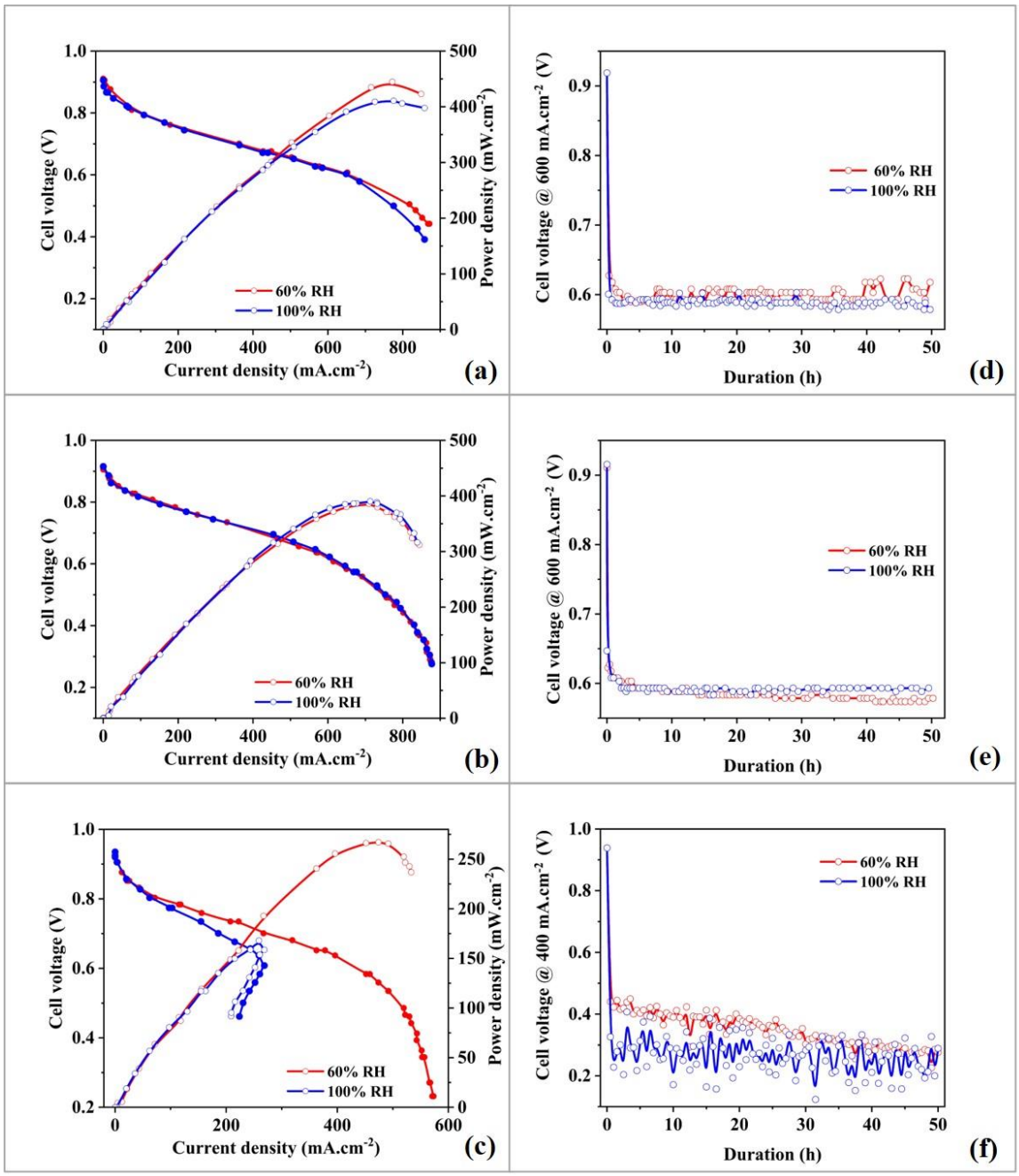

Fig. 17 - Fuel cell performance at 70 °C using H_2/air at 60 and 100% RH for 1, 2 and commercial sample, respectively (a)-(c) (b), and durability at 600 mA.cm^{-2} for samples 1 and 2 (d)-(e), and at 400 mA.cm^{-2} for the commercial sample (f).

The fuel cell performance was very poor during the durability testing of the commercial GDLs sample, this might be due to the excessive flooding. Hence the durability testing of the commercial GDLs were done at lower current density than the sample #1 and #2

4.2 Phase – 2

4.2.1 Selection criteria

The goal of the second phase was to evaluate the performance degradation of the GDLs under ASTs and to compare the two types of carbon with the commercial GDL. Hence it made sense to use the composition of the best performing sample (#2 with 30% PEG) from phase – 1 for both the carbon types for the AST study.

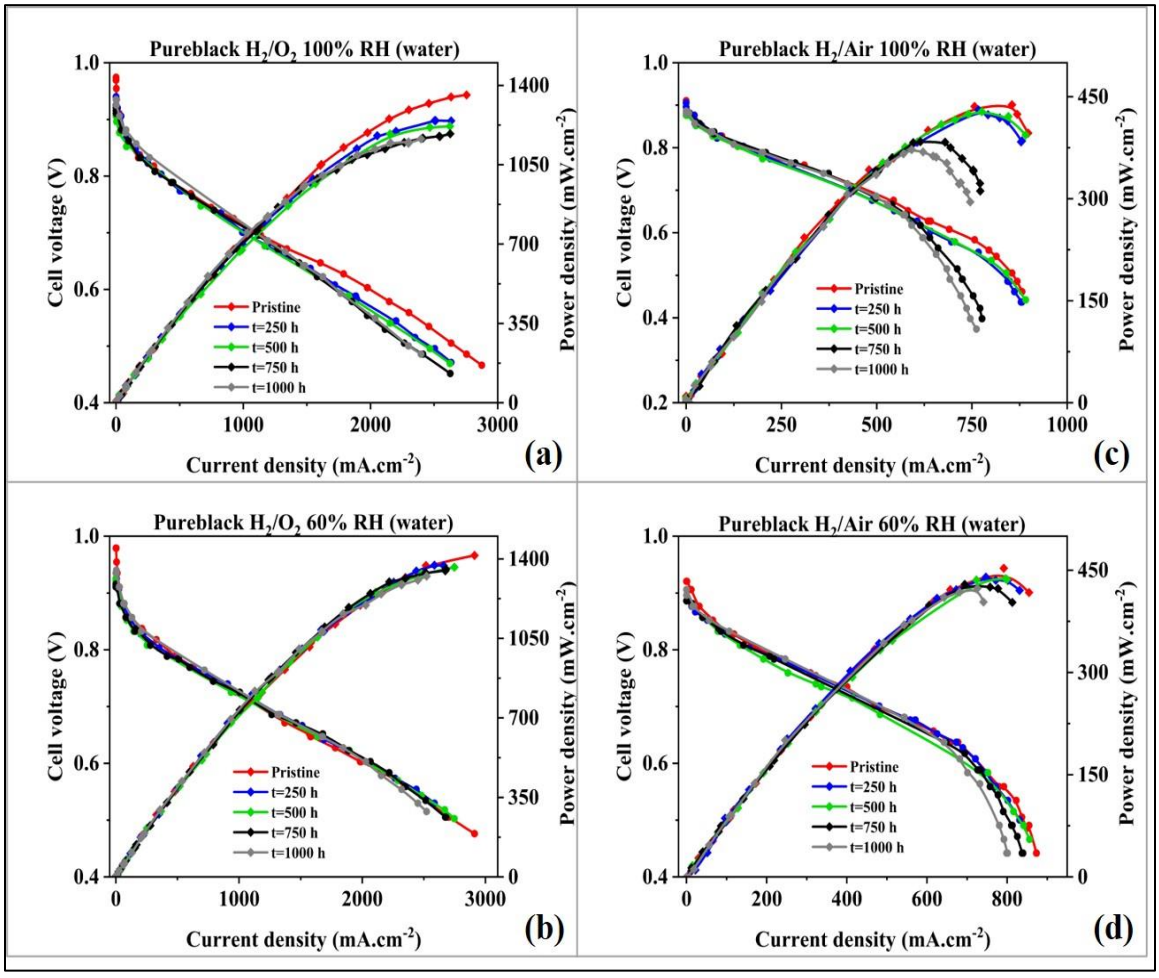

Fig. 18 - Fuel cell performance for PUREBLACK® GDL aged in water using H_2/O_2 at (a) 100%, (b) 60% RH and H_2/air at (c) 100% and (d) 60% RH.

A comparison was made between the pristine and the most degraded sample for both the PUREBLACK® and VULCAN® -based GDLs. Commercial GDLs were not selected as they showed an increase in the peak power density after degradation, this might be due to the weak structure of the GDL and its unsteady performance.

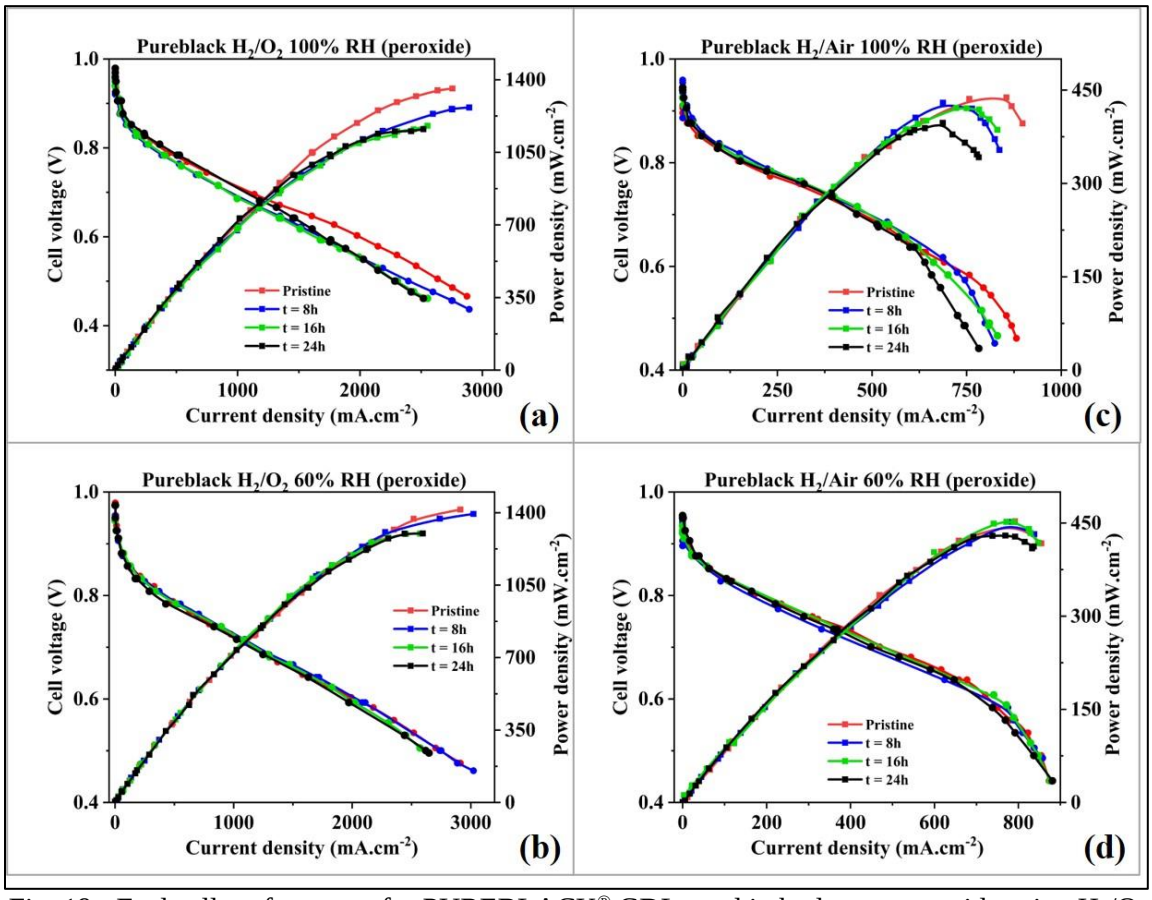

Fig. 19 - Fuel cell performance for PUREBLACK® GDL aged in hydrogen peroxide using H_2/O_2 at (a) 100%, (b) 60% RH and H_2/air at (c) 100% and (d) 60% RH.

The fuel cell performance for the PUREBLACK® based GDLs during and after the AST tests is given in Figure 18(Hydrogen peroxide) and 19(water). It is evident from the graphs that the performance at higher relative humidity conditions suffers a greater loss. Also, the performance loss increased during the ASTs for the PUREBLACK® GDLs. Similarly, figures 20(Hydrogen peroxide) and 21(water) depict the Fuel cell performance for the VULCAN® GDLs, and the performance loss was greater at high relative conditions.

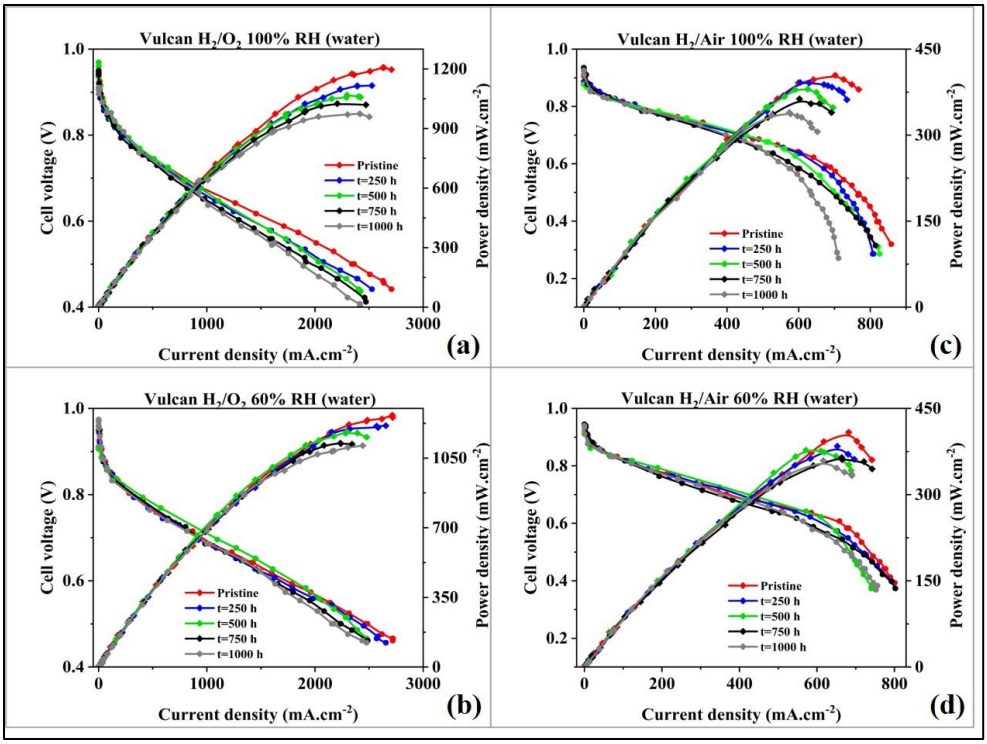

Figure 20. Fuel cell performance for VULCAN® GDL aged in water using H_2/O_2 at (a) 100%, (b) 60% RH and H_2/air at (c) 100% and (d) 60% RH.

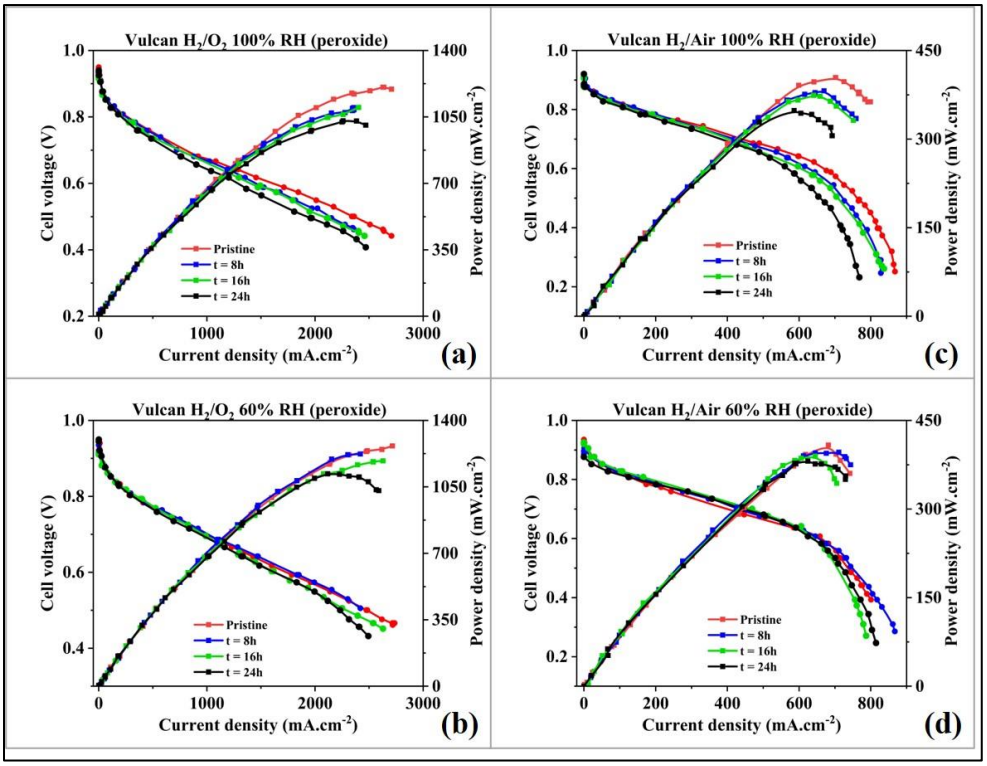

Fig. 21 - Fuel cell performance for VULCAN® GDL aged in hydrogen peroxide using H_2/O_2 at (a) 100%, (b) 60% RH and H_2/air at (c) 100% and (d) 60% RH.

PUREBLACK® performed better than VULCAN® in dry conditions. The samples which degraded the most after the ASTs were selected for further characterization.

4.2.2 Surface morphology of GDLs

Scanning Electron microscopy of the pristine samples for both PUREBLACK® (fig. 22(a)) and VULCAN® (fig. 22(b)) revealed a smooth surface as shown in figure 22. There were no signs of deep penetration or cracks, but some black spots were visible on the surface of the PUREBLACK® samples (fig. 22(b)) after immersion in hydrogen peroxide for 24 hrs. This suggests the overall pore hydrophobicity was not affected and the wettability changes might just be insignificant [76]. After 1000 h (fig. 22(c)) in warm water, the surface of the PUREBLACK® GDL looks coarse and loss of carbon can be seen which exposed the larger pores and the carbon fibers of the substrate in comparison to the pristine sample (fig. 22(a)). Noto et al. confirm the washing of carbon as carbon dioxide due to the water produced in the fuel cell [77]. Whereas changes in water management, loss of porosity, and mechanical degradation can be present in the VULCAN® GDLs as shown in figure (fig. 22(e)) due to the irregular and cracked surface resulting from surface oxidation [78]. Due to the presence of larger cracks, these effects are seen in the MPL that results in the surface roughness and are caused by the change in hydrophobicity [79], [80].

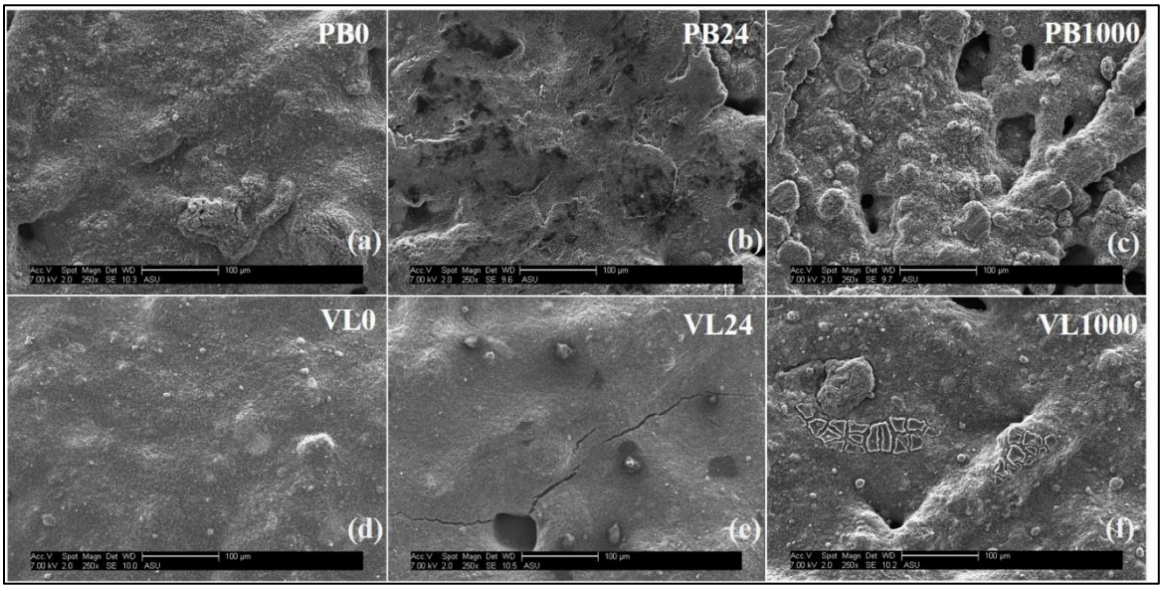

Fig. 22 - Surface morphology on GDLs with PUREBLACK® (a) pristine, (b) 24 h in hydrogen peroxide, (c) 1000 h in water, and VULCAN® -XC 72R (d) pristine, (e) 24 h in hydrogen peroxide, and (f) 1000 h in water.

4.2.3 Contact Angle

Figure 23 shows the contact angle for both the PUREBLACK® and VULCAN® GDL, and the effect of degradation can be seen as manifested by the decrease in the contact angle. The decrease in the VULCAN® GDL was greater compared to the PUREBLACK® GDL. The results for the contact angle along with the performance degradation are summarized in table 4. The main reason behind the loss in hydrophobicity of the VULCAN® GDL might be due to its structural dissimilarities (particle size, pore size, and volume) and also due to the fact, the VULCAN® carbon is not graphitized [32], [81]. Other factors including porosity change [82], [83], hydrophobic losses of the surface of MPL, improper water management [76], surface cracks increasing surface roughness [79], [80] can be attributed to the change in the hydrophobicity of the VULCAN® MPL. Decreased hydrophobicity cannot be attributed to the PTFE decomposition as SEM images (figure 22) shows no signs of PTFE loss [41], [84]. Graphitization can reduce the surface heterogeneity

while increasing the corrosion stability and hence can be attributed to the smaller loss of hydrophobicity [30], [85]–[87].

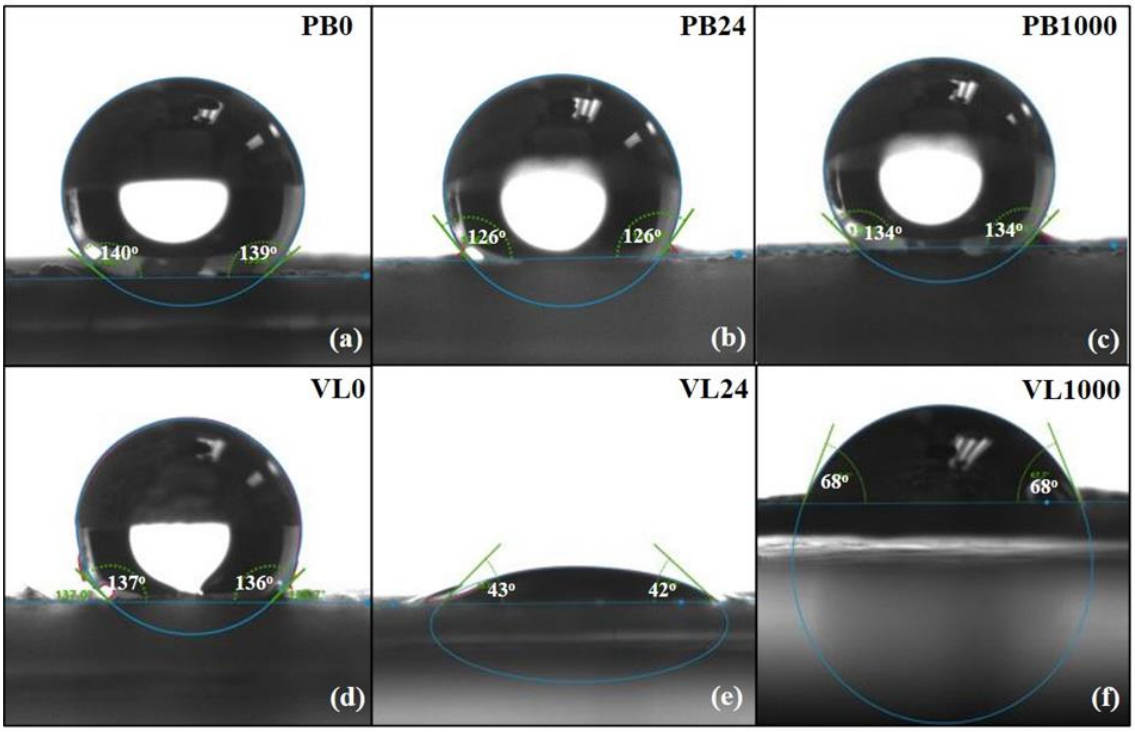

Fig. 23 - Contact angle on GDLs with PUREBLACK® (a) pristine, (b) 24 h in hydrogen peroxide, (c) 1000 h in water, and VULCAN® XC-72R (d) pristine, (e) 24 h in hydrogen peroxide, and (f) 1000 h in water.

4.2.4 Pore Size Distribution

The Pore size distribution of both samples were measure before and after the ageing to evaluate the effect of degradation and is given in figure 24.

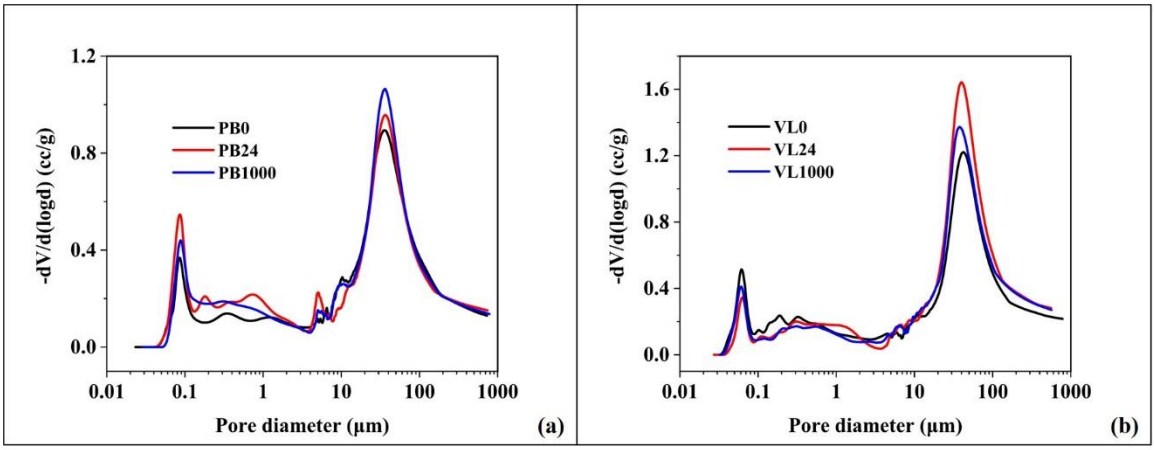

Figure 24. Pore size distribution before and after ASTs for (a) PUREBLACK® and (b) VULCAN® GDLs

It can be seen that the porosity increased compared to the pristine GDLs for all samples after ageing. This is due to carbon corrosion which was also seen in the SEM micrographs (Fig. 22). There are structural changes in all GDL samples, this is due to the increase in the macropore area in both types of carbon. Ageing can cause significant changes on the pore size distribution[88] of the GDL while having low effect on the porosity[89]. VULCAN® GDLs show a significant decrease in the micropore region after ageing, and hence can be attributed to the creation of larger pores due to the destruction of smaller pores. SEM (fig. 22 (e)) verifies the presence of larger pores on MPL and contact angle (fig. 23 (e)) verifies the hydrophobicity losscdue to carbon corrosion. As discussed earlier, larger pores facilitate water transport and the smaller pores facilitate the gas transport, but through-plane electronic conductivity decreases when the pore size increases and the gas permeability is decreased due to water filled in the cracks [33]. This reduces the fuel cell performance [59]. PUREBLACK® GDLs exhibit similar trends, however the changes in pore size distribution are not as dramatic. Also, the samples aged in hydrogen peroxide does not show any significant changes on the surface characteristics, but there was a small drop in contact angle which may be due to increased porosity [72].

Table 4. Summary of all PUREBLACK® and VULCAN® samples before and after AST.

Sample ID	Contact angle (degrees)	Total porosity (%)	Performance degradation (%)			
			O_2		Air	
			100%	60%	100%	60%
PB0	140	58	-	-	-	-
PB24	126	65	14	6	10	2
PB1000	134	60	14	5	12	2
VL0	136	63	-	-	-	-
VL24	43	69	15	12	19	11
VL1000	68	65	19	12	16	16

4.2.5 Fuel cell performance

To calculate the effect of the ASTs on the performance of the GDLs fuel cell performance was evaluated at both 60 and 100% RH in H_2/O_2 and H_2/air at 70 °C before and after AST. The results are summarized in Table 4. The fuel cell performance of both PUREBLACK® and VULCAN® before and after the AST using hydrogen peroxide is given in figure 25.

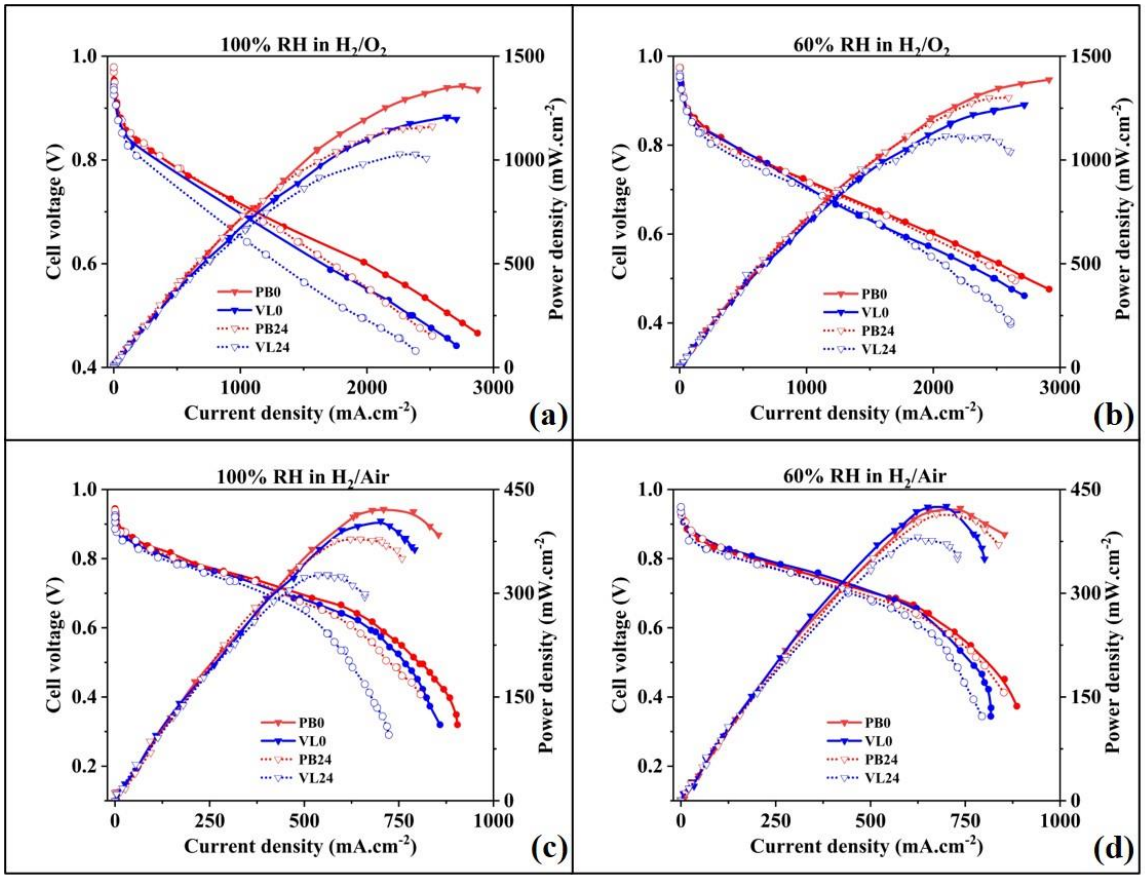

Fig. 25 - Fuel cell performance of PUREBLACK® and VULCAN® GDLs before and after AST in hydrogen peroxide in H_2/O_2 at (a) 100%, (b) 60% RH and H_2/air at (c) 100%, and (d) 60% RH.

The effect of degradation is seen for both the carbons after the tests, which is evident from the mass transport losses visible in the polarization curves at high RH (fig. 24(a) and (c)). Grigoria A. et al. showed the durability and performance of PUREBLACK® with 30%

PEG as the pore-forming agent, this configuration showed better water management preventing flooding at both 60 and 100% RH [90]. This might be due to the pore size distribution and the surface characteristics of the GDL, which is similar to the results of this study.

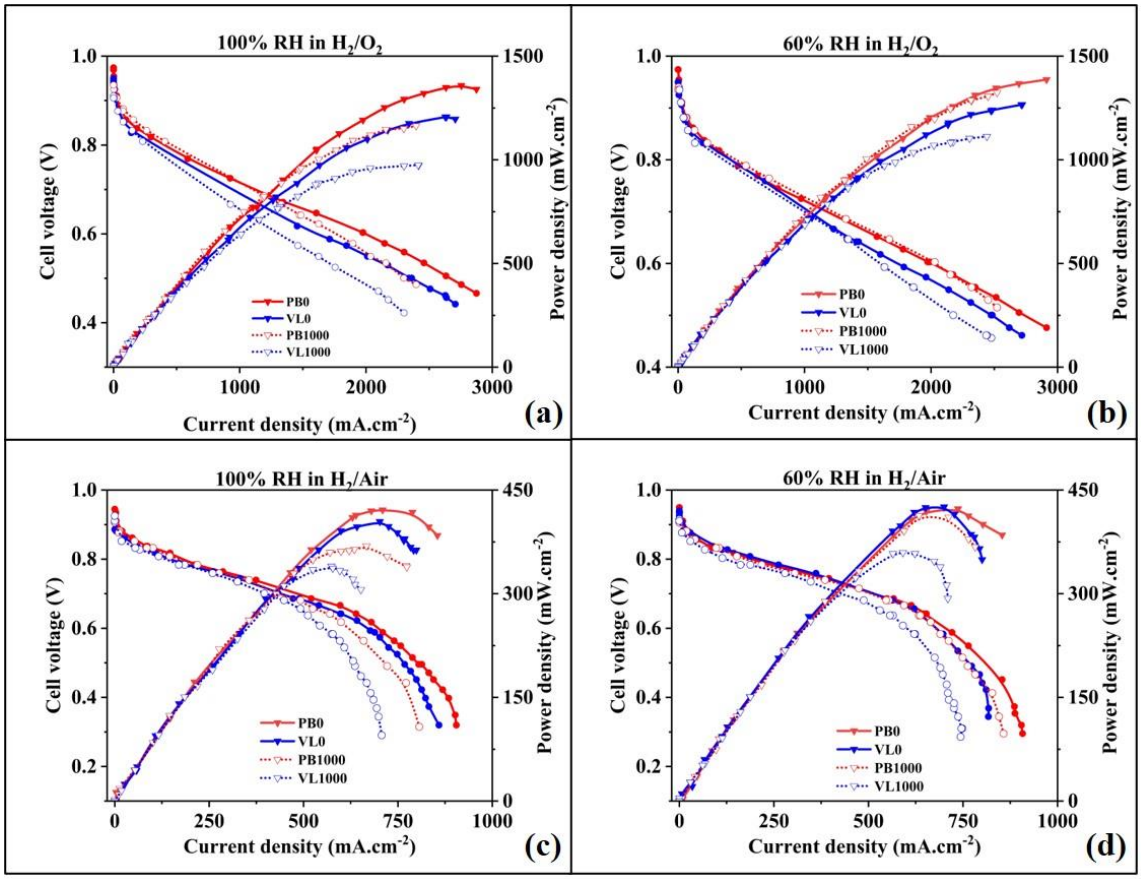

Fig. 26 - Fuel cell performance of PUREBLACK® and VULCAN® GDLs before and after AST in water in H_2/O_2 at (a) 100%, (b) 60% RH and H_2/air at (c) 100%, and (d) 60% RH

A drop of 14% in H_2/O_2 and 10% in H_2/air in the fuel cell performance at high RH for PUREBLACK® GDL after ageing in hydrogen peroxide for 24 h was recorded. Flooding is the main reason why the fuel cell performance was so low after ageing in hydrogen peroxide, this is because it facilitates the chemical corrosion of carbon, which

causes improper water management in the GDLs [58], [91]. At lower current densities mass transport losses are observed, due to the voltage drop. This happens when the fuel cell is flooded and produces water that covers the GDL pores which inhibits the flow of reactant gases to the catalyst layer [92], [93]. This is the reason for the mass transport loss in the PUREBLACK® GDL at high RH conditions under the current density of 1500 and 600 $mA.cm^{-2}$ in H_2/O_2 and H_2/air, respectively. The fuel cell performance degradation is greater in the VULCAN® GDL (see table 4) and mass transport losses are visible at around 1000 and 400 $mA.cm^{-2}$ in H_2/O_2 and H_2/air, respectively, this shows that carbon corrosion affects VULCAN® more and hence creates more imperfections in its GDL structure [94], [95].

Figure 26 shows the fuel cell performance for both GDLs before and after AST in water and table 4 presents the summary of the percentage loss. VULCAN® shows more mass transport loss at higher RH conditions for both H_2/O_2 and H_2/air, this is also seen in PUREBLACK® based GDLs. But the performance degradation for VULCAN® was higher than PUREBLACK® GDLs, this shows the greater susceptibility to carbon corrosion for VULCAN® . The flooding effect caused by GDL degradation is less in low RH conditions than in wet conditions, but the degradation rate for VULCAN® tends to be higher in all conditions as compared to PUREBLACK®. As mentioned earlier this can be attributed to the graphitization of the PUREBLACK® which provides carbon corrosion resistance, whereas VULCAN® is non-graphitized leading to higher carbon carrion.

4.2.5 Durability

For the second phase of the research unaged samples for both the PUREBLACK® and VULCAN® GDLs were selected for the durability test, to compare the performance of the two carbon types. The conditions for the durability tests were the same as the phase

– 1, i.e., H_2/air was used as the oxidant, the current density was kept constant at 600 mA.cm^{-2}. To achieve ideal membrane hydration the MEAs were evaluated at 100% RH initially and then at 60% RH. The performance of both GDLs is presented in figure 27.

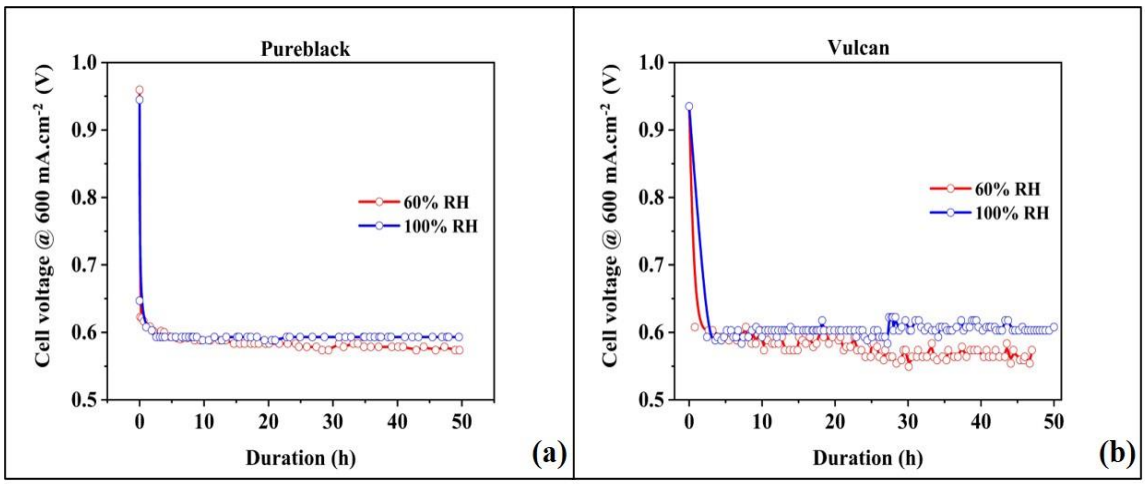

Fig. 27 – Durability test using H_2/air for 50h at 100% and 50 h at 60% RH at 70 °C and constant current density of 600 mA.cm^{-2} for pristine (a) PUREBLACK® and (b) VULCAN® GDLs.

The graphs show that the PUREBLACK® is much more constant and the voltage drop after 50hrs at 100% RH was negligible, whereas at 60% RH it was noticeable. However, for VULCAN® , there are irregularities in the graph which shows the voltage irregularities that can be due to the high stability of the water droplets. This is because of the loss of hydrophobicity which is caused by the channel clogging as it makes it difficult to separate the water droplet from the GDL surface [41].

CHAPTER 5

CONCLUSION

The study was conducted in 2 parts. Phase – 1 of the research was conducted to find the best composition of the GDL with and without pore-forming agent using PUREBLACK® carbon. The second phase of the research was to extend the research to two sets of carbon types and including VULCAN® carbon and comparing with PUREBLACK® and commercial GDLs and testing for the durability of each type using the accelerated stress tests.

Microporous layers were fabricated on the carbon paper substrate using different types of carbon and commercial GDL (AvCarb GDS 2120) and were evaluated using a single cell PEM fuel cell. H_2/O_2 and H_2/air were used as the oxidants under 60 and 100% RH conditions. SEM was used to study the surface morphology, contact angle measurements were done to assess the surface wettability characteristics and mercury intrusion porosimetry was used to evaluate the pore size distribution. During phase – 1, sample – 2 (with 30% PEG) performed best overall at both RH conditions and both oxidants, (with the highest pore volume of 1.72 $cc.g^{-1}$) the fuel cell performance was 444 and 432 $mWcm^{-2}$ at 60 and 100% RH respectively using air. The final confirmation of the better performance of the PUREBLACK® GDL was the durability testing (at 600 $mAcm^{-2}$), where after 50h at 100% RH and 50 h at 60% RH conditions, the performance was better compared to the commercial GDL. This proved that for stable performance of the fuel cell optimum pore size distribution and the crack-free hydrophobic characteristics of the GDL are required.

For Phase – 2, One single composition (30% PEG) was used for all GDL samples and tested for accelerated tests using hydrogen peroxide and warm water. The GDL with PUREBLACK® carbon performed best overall. This was attributed to the graphitized core of the carbon in PUREBLACK® which prevents the corrosion of carbon by the dissolution effect. The performance degradation after the AST in hydrogen peroxide was 10 and 2% at 100 and 60% RH respectively using air as an oxidant. Whereas, in VULCAN® , it was 19 and 11% at 100 and 60% RH, respectively. Similarly, in warm water, the performance of PUREBLACK® was better than the VULCAN® and commercial GDLs.

REFERENCES

[1] Z. Adam and H. Bahar, *Global Energy Review 2020*. Internation Energy Agency, 2020.

[2] E. Sugawara and H. Nikaido, *EIA energy outlook 2020*, vol. 58, no. 12. 2019.

[3] M. Suha Yazici, "Hydrogen and fuel cell activities at UNIDO-ICHET," *Int. J. Hydrogen Energy*, vol. 35, no. 7, pp. 2754–2761, 2010.

[4] F. Barbir and S. Yazici, "Status and devlopment of PEM fuel cell technology," *Int. J. Energy Res.*, vol. 32, pp. 369–378, 2008.

[5] I. R. E. A. IRENA, *Hydrogen : a Renewable Energy Perspective*, no. September. 2019.

[6] D. Anderson, "David Sandborn Scott, Smelling Land: The Hydrogen Defense Against Climate Catastrophe," *Environmentalist*, vol. 28, no. 4, pp. 494–495, 2008.

[7] I. Dincer and C. Acar, "Smart energy solutions with hydrogen options," *Int. J. Hydrogen Energy*, vol. 43, no. 18, pp. 8579–8599, 2018.

[8] J. Larminie and A. Dicks, *Fuel Cell Systems Explained*, Second. John wiley & sons, 2003.

[9] W. R. Grove, *The correlation of physical forces*, 6th ed. Longsman, Green & Co., London, 1874.

[10] F. Barbir, *PEM Fuel cells: Theory and Practice*. Academic press, 2005.

[11] J. Zhang, *PEM Fuel Cell Electrocatalysts and Catalyst Layers Fundamentals and applications*. Springer, London, 2008.

[12] E. B. Yeager and A. J. Appleby, "Solid Polymer electrolyte Fuel Cells," *Energy*, vol. 11, pp. 137–152, 1986.

[13] T. Chen, S. Liu, J. Zhang, and M. Tang, "Study on the characteristics of GDL with different PTFE content and its effect on the performance of PEMFC," *Int. J. Heat Mass Transf.*, vol. 128, pp. 1168–1174, 2019.

[14] S. Shimpalee, U. Beuscher, and J. W. Van Zee, "Analysis of GDL flooding effects on PEMFC performance," *Electrochim. Acta*, vol. 52, no. 24, pp. 6748–6754, 2007.

[15] L. R. Jordan, A. K. Shukla, T. Behrsing, N. R. Avery, B. C. Muddle, and M. Forsyth, "Effect of diffusion-layer morphology on the performance of polymer

electrolyte fuel cells operating at atmospheric pressure," *J. Appl. Electrochem.*, vol. 30, no. 6, pp. 641–646, 2000.

[16] M. Neergat and A. K. Shukla, "Effect of diffusion-layer morphology on the performance of solid-polymer-electrolyte direct methanol fuel cells," *J. Power Sources*, vol. 104, no. 2, pp. 289–294, 2002.

[17] L. Cindrella *et al.*, "Gas diffusion layer for proton exchange membrane fuel cells-A review," *J. Power Sources*, vol. 194, no. 1, pp. 146–160, 2009.

[18] S. Park, J. W. Lee, and B. N. Popov, "A review of gas diffusion layer in PEM fuel cells: Materials and designs," *Int. J. Hydrogen Energy*, vol. 37, no. 7, pp. 5850–5865, 2012.

[19] T. H. Ko, Y. K. Liao, and C. H. Liu, "Effects of fabricated gas diffusion layers with different reinforce materials in proton exchange membrane fuel cell (PEMFC)," *Energy and Fuels*, vol. 22, no. 6, pp. 4092–4097, 2008.

[20] M. F. Mathias, J. Roth, J. Fleming, and W. Lehnert, "Diffusion media materials and characterisation," *Handb. Fuel Cells*, vol. 3, 2010.

[21] G. G. Park, Y. J. Sohn, T. H. Yang, Y. G. Yoon, W. Y. Lee, and C. S. Kim, "Effect of PTFE contents in the gas diffusion media on the performance of PEMFC," *J. Power Sources*, vol. 131, no. 1–2, pp. 182–187, 2004.

[22] C. I, Y. Y, and X. X, "Gas diffusion electrodes based on poly(vinylidene fluoride) carbon blends.," 5783325, 1981.

[23] C. Lim and C. Y. Wang, "Effects of hydrophobic polymer content in GDL on power performance of a PEM fuel cell," *Electrochim. Acta*, vol. 49, no. 24, pp. 4149–4156, 2004.

[24] H. Nakajima, T. Konomi, and T. Kitahara, "Direct water balance analysis on a polymer electrolyte fuel cell (PEFC): Effects of hydrophobic treatment and micro-porous layer addition to the gas diffusion layer of a PEFC on its performance during a simulated start-up operation," *J. Power Sources*, vol. 171, no. 2, pp. 457–463, 2007.

[25] S. Park, J. W. Lee, and B. N. Popov, "Effect of PTFE content in microporous layer on water management in PEM fuel cells," *J. Power Sources*, vol. 177, no. 2, pp. 457–463, 2008.

[26] A. Z. Weber and J. Newman, "Effects of Microporous Layers in Polymer Electrolyte Fuel Cells," *J. Electrochem. Soc.*, vol. 152, no. 4, p. A677, 2005.

[27] K. Jiao and B. Zhou, "Effects of electrode wettabilities on liquid water behaviours in PEM fuel cell cathode," *J. Power Sources*, vol. 175, no. 1, pp. 106–119, 2008.

[28] R. Omrani and B. Shabani, “Gas diffusion layer modifications and treatments for improving the performance of proton exchange membrane fuel cells and electrolysers: A review,” *Int. J. Hydrogen Energy*, vol. 42, no. 47, pp. 28515–28536, 2017.

[29] E. A. Wargo, V. P. Schulz, A. Çeçen, S. R. Kalidindi, and E. C. Kumbur, “Resolving macro- and micro-porous layer interaction in polymer electrolyte fuel cells using focused ion beam and X-ray computed tomography,” *Electrochim. Acta*, vol. 87, pp. 201–212, 2013.

[30] I. V. Barsukov, M. A. Gallego, and J. E. Doninger, “Novel materials for electrochemical power sources - Introduction of PUREBLACK® Carbons,” *J. Power Sources*, vol. 153, no. 2, pp. 288–299, 2006.

[31] A. M. Kannan, L. Cindrella, and L. Munukutla, “Functionally graded nano-porous gas diffusion layer for proton exchange membrane fuel cells under low relative humidity conditions,” *Electrochim. Acta*, vol. 53, no. 5, pp. 2416–2422, 2008.

[32] A. M. Kannan, A. Menghal, and I. V. Barsukov, “Gas diffusion layer using a new type of graphitized nano-carbon PUREBLACK® for proton exchange membrane fuel cells,” *Electrochem. commun.*, vol. 8, no. 5, pp. 887–891, 2006.

[33] M. V Williams, E. Begg, L. Bonville, and H. R. Kunz, “Characterization of Gas Diffusion Layers for PEMFC,” pp. 1173–1180, 2004.

[34] N. Perez, *Electrochemistry and corrosion science : Kinetics of Activation Polarization*. Springer, Cham, 2016.

[35] D. Myers and R. Borup, “Durability Working Group | Department of Energy.” https://www.energy.gov/eere/fuelcells/durability-working-group (accessed Feb. 16, 2021).

[36] D. L. Wood and R. L. Borup, “Estimation of Mass-Transport Overpotentials during Long-Term PEMFC Operation,” *J. Electrochem. Soc.*, vol. 157, no. 8, p. B1251, 2010.

[37] Y. Hiramitsu *et al.*, “Influence of humidification on deterioration of gas diffusivity in catalyst layer on polymer electrolyte fuel cell,” *J. Power Sources*, vol. 195, no. 2, pp. 435–444, 2010.

[38] M. Bosomoiu, G. Tsotridis, and T. Bednarek, “Study of effective transport properties of fresh and aged gas diffusion layers,” *J. Power Sources*, vol. 285, pp. 568–579, 2015.

[39] C. A. Reiser *et al.*, “A reverse-current decay mechanism for fuel cells,” *Electrochem. Solid-State Lett.*, vol. 8, no. 6, pp. 273–276, 2005.

[40] J. Park, H. Oh, T. Ha, Y. Il Lee, and K. Min, “A review of the gas diffusion layer

in proton exchange membrane fuel cells: Durability and degradation," *Appl. Energy*, vol. 155, pp. 866–880, 2015.

[41] T. Ha *et al.*, "Experimental study on carbon corrosion of the gas diffusion layer in polymer electrolyte membrane fuel cells," *Int. J. Hydrogen Energy*, vol. 36, no. 19, pp. 12436–12443, 2011.

[42] S. G. Kandlikar, M. L. Garofalo, and Z. Lu, "Water management in a PEMFC: Water transport mechanism and material degradation in gas diffusion layers," *Fuel Cells*, vol. 11, no. 6, pp. 814–823, 2011.

[43] F. Lapicque, M. Belhadj, C. Bonnet, J. Pauchet, and Y. Thomas, "A critical review on gas diffusion micro and macroporous layers degradations for improved membrane fuel cell durability," *J. Power Sources*, vol. 336, pp. 40–53, 2016.

[44] J. Cho *et al.*, "Analysis of transient response of a unit proton-exchange membrane fuel cell with a degraded gas diffusion layer," *Int. J. Hydrogen Energy*, vol. 36, no. 10, pp. 6090–6098, 2011.

[45] G. Chen, H. Zhang, H. Ma, and H. Zhong, "Electrochemical durability of gas diffusion layer under simulated proton exchange membrane fuel cell conditions," *Int. J. Hydrogen Energy*, vol. 34, no. 19, pp. 8185–8192, 2009.

[46] J. Chlistunoff, J. R. Davey, K. C. Rau, R. Mukundan, and R. L. Borup, "PEMFC Gas Diffusion Media Degradation Determined by Acid-Base Titrations," *ECS Trans.*, vol. 50, no. 2, pp. 521–529, 2013.

[47] Y. Hiramitsu, H. Sato, K. Kobayashi, and M. Hori, "Controlling gas diffusion layer oxidation by homogeneous hydrophobic coating for polymer electrolyte fuel cells," *J. Power Sources*, vol. 196, no. 13, pp. 5453–5469, 2011.

[48] T. Arlt, M. Klages, M. Messerschmidt, J. Scholta, and I. Manke, "Influence of artificially aged gas diffusion layers on the water management of polymer electrolyte membrane fuel cells analyzed with in-operando synchrotron imaging," *Energy*, vol. 118, pp. 502–511, 2017.

[49] D. Spernjak, J. D. Fairweather, T. Rockward, R. Mukundan, and R. Borup, "Characterization of Carbon Corrosion in a Segmented PEM Fuel Cell," *ECS Trans.*, pp. 47–741, 2011.

[50] X. Z. Yuan, H. Li, S. Zhang, J. Martin, and H. Wang, "A review of polymer electrolyte membrane fuel cell durability test protocols," *J. Power Sources*, vol. 196, no. 22, pp. 9107–9116, 2011.

[51] S. J. Lim *et al.*, "Investigation of freeze/thaw durability in polymer electrolyte fuel cells," *Int. J. Hydrogen Energy*, vol. 35, no. 23, pp. 13111–13117, 2010.

[52] A. Wang, W. Liu, N. Ren, J. Zhou, and S. Cheng, "Key factors affecting microbial

anode potential in a microbial electrolysis cell for H2 production," *Int. J. Hydrogen Energy*, vol. 35, no. 24, pp. 13481–13487, 2010.

[53] "FCTT AST and Polarization Curve Protocols for PEMFCs," U.S. DRIVE Fuel Cell Tech Team, 2013.

[54] P. K. Das, A. Grippin, A. Kwong, and A. Z. Weber, "Liquid-Water-Droplet Adhesion-Force Measurements on Fresh and Aged Fuel-Cell Gas-Diffusion Layers," *J. Electrochem. Soc.*, vol. 159, no. 5, pp. B489–B496, 2012.

[55] D. Wood, J. Xie, S. Pacheco, R. Borup, and J. Davey, "Durability issues of the PEMFC GDL and MEA under steady-state and drive-cycle operating conditions," *Los Alamos Natl. Lab.*, 2004.

[56] E. Passalacqua, F. Lufrano, G. Squadrito, A. Patti, and L. Giorgi, "Nafion content in the catalyst layer of polymer electrolyte fuel cells: Effects on structure and performance," *Electrochim. Acta*, vol. 46, no. 6, pp. 799–805, 2001.

[57] J. Liu, C. Yang, C. Liu, F. Wang, and Y. Song, "Design of pore structure in gas diffusion layers for oxygen depolarized cathode and their effect on activity for oxygen reduction reaction," *Ind. Eng. Chem. Res.*, vol. 53, no. 14, pp. 5866–5872, 2014.

[58] H. Liu *et al.*, "Accelerated Degradation of Polymer Electrolyte Membrane Fuel Cell Gas Diffusion Layers," *J. Electrochem. Soc.*, vol. 164, no. 7, pp. F695–F703, 2017.

[59] X. L. Wang *et al.*, "Micro-porous layer with composite carbon black for PEM fuel cells," vol. 51, pp. 4909–4915, 2006.

[60] J. Lobato, P. Cañizares, M. A. Rodrigo, D. Ubeda, F. J. Pinar, and J. J. Linares, "Optimisation of the Microporous Layer for a Polybenzimidazole-Based High Temperature PEMFC–Effect of Carbon Content.pdf," *Fuel Cells, Wiley-VCH Verlag*, vol. 10(5), p. 770, 2010.

[61] S. B. Park, S. Kim, Y. Il Park, and M. H. Oh, "Fabrication of GDL microporous layer using PVDF for PEMFCs," *J. Phys. Conf. Ser.*, vol. 165, 2009.

[62] J. H. Lin, W. H. Chen, S. H. Su, Y. J. Su, and T. H. Ko, "Washing experiment of the gas diffusion layer in a proton-exchange membrane fuel cell," *Energy and Fuels*, vol. 22, no. 4, pp. 2533–2538, 2008.

[63] J. H. Chun, D. H. Jo, S. G. Kim, S. H. Park, C. H. Lee, and S. H. Kim, "Improvement of the mechanical durability of micro porous layer in a proton exchange membrane fuel cell by elimination of surface cracks," *Renew. Energy*, vol. 48, pp. 35–41, 2012.

[64] G. Lin and T. Van Nguyen, "Effect of Thickness and Hydrophobic Polymer

Content of the Gas Diffusion Layer on Electrode Flooding Level in a PEMFC," *J. Electrochem. Soc.*, vol. 152, no. 10, p. A1942, 2005.

[65] U. Pasaogullari and C. Y. Wang, "Liquid Water Transport in Gas Diffusion Layer of Polymer Electrolyte Fuel Cells," *J. Electrochem. Soc.*, no. 151:A399, 2004.

[66] F. S. Nanadegani, E. N. Lay, and B. Sunden, "Effects of an MPL on water and thermal management in a PEMFC," *Int. J. Energy Res.*, vol. 43, no. 1, pp. 274–296, 2019.

[67] B. Larbi, W. Alimi, R. Chouikh, and A. Guizani, "Effect of porosity and pressure on the PEM fuel cell performance," *Int. J. Hydrogen Energy*, vol. 38, no. 20, pp. 8542–8549, 2013.

[68] E. Passalacqua, G. Squadrito, F. Lufrano, A. Patti, and L. Giorgi, "Effects of the diffusion layer characteristics on the performance of polymer electrolyte fuel cell electrodes," *J. Appl. Electrochem.*, vol. 31, no. 4, pp. 449–454, 2001.

[69] H. K. Lee, J. H. Park, D. Y. Kim, and T. H. Lee, "A study on the characteristics of the diffusion layer thickness and porosity of the PEMFC," *J. Power Sources*, vol. 131, no. 1–2, pp. 200–206, 2004.

[70] FSE center, "Procedure for performing PEM single cell testing," *Test Protocol for Cell Performance Tests Performed US Department of energy*, 2009.

[71] Q. Shen *et al.*, "The voltage characteristics of proton exchange membrane fuel cell (PEMFC) under steady and transient states," *J. Power Sources*, vol. 179, no. 1, pp. 292–296, 2008.

[72] J. E. Owejan, P. T. Yu, and R. Makharia, "Mitigation of Carbon Corrosion in Microporous Layers in PEM Fuel Cells," *ECS Trans.*, vol. 11, no. 1, pp. 1049–1057, 2019.

[73] A. P. Young, J. Stumper, and E. Gyenge, "Characterizing the Structural Degradation in a PEMFC Cathode Catalyst Layer: Carbon Corrosion," *J. Electrochem. Soc.*, vol. 156, no. 8, p. B913, 2009.

[74] S. C. Ball, S. L. Hudson, D. Thompsett, and B. Theobald, "An investigation into factors affecting the stability of carbons and carbon supported platinum and platinum/cobalt alloy catalysts during 1.2 V potentiostatic hold regimes at a range of temperatures," *J. Power Sources*, vol. 171, no. 1, pp. 18–25, 2007.

[75] D. A. Stevens, M. T. Hicks, G. M. Haugen, and J. R. Dahn, "Ex situ and in situ stability studies of PEMFC catalysts: effect of carbon type and humidification on degradation of the carbon," *J. Electrochem. Soc.*, vol. 152, no. 12, p. A2309, 2005.

[76] S. Komini Babu, T. O'Brien, M. J. Workman, M. Wilson, R. Mukundan, and R. Borup, "Editors' Choice—Diffusion Media for Cation Contaminant Transport

Suppression into Fuel Cell Electrodes," *J. Electrochem. Soc.*, vol. 168, no. 2, p. 024501, 2021.

[77] H. Noto, M. Kondo, Y. Otake, and M. Kato, "Development of fuel cell hybrid vehicle by Toyota -durability-," *SAE Tech. Pap.*, 2009.

[78] D. Spernjak, J. Fairweather, R. Mukundan, T. Rockward, and R. L. Borup, "Influence of the microporous layer on carbon corrosion in the catalyst layer of a polymer electrolyte membrane fuel cell," *J. Power Sources*, vol. 214, pp. 386–398, 2012.

[79] E. L. Decker, B. Frank, Y. Suo, and S. Garoff, "Physics of contact angle measurement," vol. 156, pp. 177–189, 1999.

[80] F. Y. H. Lin, D. Li, and A. W. Neumann, "Effect of surface roughness on the dependence of contact angles on drop size," *Journal of Colloid And Interface Science*, vol. 159, no. 1. pp. 86–95, 1993, doi: 10.1006/jcis.1993.1300.

[81] G. A. Gruver, "The Corrosion of Carbon Black in Phosphoric Acid," *J. Electrochem. Soc.*, vol. 125, no. 10, pp. 1719–1720, 1978.

[82] D. L. Wood and R. L. Borup, "Durability aspects of gas-diffusion and microporous layers," *Polym. Electrolyte Fuel Cell Durab.*, pp. 159–195, 2009.

[83] K. H. Kangasniemi, D. A. Condit, and T. D. Jarvi, "Characterization of Vulcan Electrochemically Oxidized under Simulated PEM Fuel Cell Conditions," *J. Electrochem. Soc.*, vol. 151, no. 4, p. E125, 2004.

[84] and R. B. Wood, David, John Davey, Plamen Atanassov, "PEMFC Component Characterization and Its Relationship to Mass-Transport Overpotentials during Long-Term Testing," *ECS Trans.*, 2006.

[85] H. M. Yu, C. Ziegler, M. Oszcipok, M. Zobel, and C. Hebling, "Hydrophilicity and hydrophobicity study of catalyst layers in proton exchange membrane fuel cells," *Electrochim. Acta*, vol. 51, no. 7, pp. 1199–1207, 2006.

[86] S. Maass, F. Finsterwalder, G. Frank, R. Hartmann, and C. Merten, "Carbon support oxidation in PEM fuel cell cathodes," *J. Power Sources*, vol. 176, no. 2, pp. 444–451, 2008, doi: 10.1016/j.jpowsour.2007.08.053.

[87] E. Auer, A. Freund, J. Pietsch, and T. Tacke, "Carbons as supports for industrial precious metal catalysts," *Appl. Catal. A Gen.*, vol. 173, no. 2, pp. 259–271, 1998, doi: 10.1016/S0926-860X(98)00184-7.

[88] C. Lee and W. Mérida, "Gas diffusion layer durability under steady-state and freezing conditions," *J. Power Sources*, vol. 164, no. 1, pp. 141–153, 2007.

[89] C. S. Kong, D. Y. Kim, H. K. Lee, Y. G. Shul, and T. H. Lee, "Influence of pore-

size distribution of diffusion layer on mass-transport problems of proton exchange membrane fuel cells," *J. Power Sources*, vol. 108, no. 1–2, pp. 185–191, 2002.

[90] G. Athanasaki *et al.*, "Design and development of gas diffusion layers with pore forming agent for proton exchange membrane fuel cells at various relative humidity conditions," *Int. J. Hydrogen Energy*, vol. 46, no. 9, pp. 6835–6844, 2021.

[91] X. Zhang, Y. Yang, X. Zhang, L. Guo, and H. Liu, "Increase of Mass Transport Loss in Porous Media Caused By Carbon Corrosion in Pem Fuel," no. May, pp. 9–11, 2018.

[92] S. M. Baek, S. G. Koh, K. N. Kim, J. H. Kang, J. H. Nam, and C. J. Kim, "A numerical study on the performance of polymer electrolyte membrane fuel cells due to the variation in gas diffusion layer permeability," *J. Mech. Sci. Technol.*, vol. 25, no. 2, pp. 457–467, 2011.

[93] M. G. George *et al.*, "Accelerated Degradation of Polymer Electrolyte Membrane Fuel Cell Gas Diffusion Layers," *J. Electrochem. Soc.*, vol. 164, no. 7, pp. F714–F721, 2017, doi: 10.1149/2.0091707jes.

[94] P. K. Mohanta, F. Regnet, and L. Jörissen, "Graphitized Carbon: A promising stable cathode catalyst support material for long term PEMFC applications," *Materials (Basel).*, vol. 11, no. 6, 2018.

[95] H. S. Oh, K. H. Lim, B. Roh, I. Hwang, and H. Kim, "Corrosion resistance and sintering effect of carbon supports in polymer electrolyte membrane fuel cells," *Electrochim. Acta*, vol. 54, no. 26, pp. 6515–6521, 2009.